UNIVERZA V LJUBLJANI

FAKULTETA ZA FARMACIJO

SIMONA RUPNIK

MAGISTRSKA NALOGA

MAGISTRSKI ŠTUDIJSKI PROGRAM INDUSTRIJSKA FARMACIJA

Ljubljana, 2015

UNIVERZA V LJUBLJANI

FAKULTETA ZA FARMACIJO

SIMONA RUPNIK

TUNING OF MECHANICAL PROPERTIES OF POLYLACTIC ACID BASED ELASTOMERS WITH CHEMICAL CROSS-LINKING

NAČRTOVANJE MEHANSKIH LASTNOSTI ELASTOMEROV POLIMLEČNE KISLINE S KEMIJSKIM PREMREŽEVANJEM

MAGISTRSKA NALOGA

Ljubljana, 2015

Research study was performed at the Institute of Biomolecules Max Mousseron (IBMM-Institut des Biomolécules Max Mousseron, Team Artificial Biopolymers) in Montpellier, France and at the University of Montpellier 1, Faculty of Pharmacy under co-supervision of Assist. Prof. Dr Benjamin Nottelet and the mentorship of Assist. Prof. Dr. Biljana Janković.

Acknowledgement

I would like to express my gratitude to Dr. Benjamin Nottelet for my engagement in this project and helping me throughout my study in Montpellier.

Velika zahvala, da je to delo dokončano, pa gre doc. dr. Biljani Janković, ki me je med samim pisanjem diplomske naloge usmerjala, si v ta namen vzela svoj čas in mi bila v veliko pomoč.

Zahvaljujem se družini in prijateljem za vse vzpodbudne besede tekom študija.

Statement

I declare that I have made this thesis independently and under cosupervision of Dr. Benjamin Nottelet and the mentorship of Assist. Prof. Dr. Biljana Janković.

Ljubljana, avgust 2015 Simona Rupnik

Predsednik diplomske komisije: izr. prof. dr. Janez Ilaš

Član diplomske komisije: doc. dr. Tomaž Bratkovič

Table of Contents

ABSTRACT

Tissue engineering is an interdisciplinary science that includes biology, medicine, material science, pharmacy, etc. The main purpose of tissue engineering is to prepare appropriate scaffolds, which are able to imitate native tissue in order to replace the damaged structures or to support the cell growth (imitate the healing processes). Tissue engineering scaffolds are three-dimensional surroundings prepared from natural and synthetic materials. PLA-based biodegradable soft elastomers are one of the materials that can be used as supporting material for bioengineering. In this study, several thermoset biodegradable photo cross-linked poly(lactide)-poly(ethylene glycol)-poly(lactide) (PLA-PEG-PLA) elastomers with different molecular weight were prepared. The preparation of those elastomers was based on the modification of ratio of ethylene oxide and lactyl units (EO/LA ratio) as well as on selection of used cross-linkers. Pentaerythritol tetra(3-mercaptopropionate) (PETMP) and diallyl disulfide (DD) were used as tested cross-linkers. E_{4000} elastomers were prepared from methacrylated triblock copolymers with number average molecular weight around 4000 g/mol. E_{12000} elastomers were prepared in the same way with triblock copolymers having number average molecular weight around 12000 g/mol. Mechanical properties have been evaluated in dry and in hydrated state by tensile test. According to the results, the molecular weight, molecular packing and the crystalline/amorphous structure have major impact on mechanical properties when compared to cross-linker structure. DD-based E_{4000} elastomers are stiffer due to more ordered structure of the smaller polymeric chains and their more compact layering in the scaffold structure. Only for $E_{4000\text{-}1}$ (elastomer without added cross-linker) and $E_{12000\text{-}2}$ (elastomer based on PETMP), significant difference was noticeable in hydrated state. Degradation profile can be tailored by amphiphilic balance of triblock copolymer and hydrophilicity/hydrophobicity of selected cross-linker. The degradation test showed that the elastomers with higher EO/LA ratio and hydrophilic cross-linker expressed the highest weight loss during 3 months. Results from tensile tests indicate that prepared elastomers can be used for replacement of soft natural tissues such as vascular vessels and nasal cartilage.

Keywords: *tissue engineering, elastomers, Young's modulus, biodegradation, cross-linkers*

RAZŠIRJEN POVZETEK

Današnjega sveta si brez polimerov skoraj več ne moremo predstavljati, saj imajo zelo širok spekter uporabe. V zadnjem času je pozornost še posebej usmerjana na možnosti njihove uporabe v zdravstvu in farmaciji. V farmaciji so še posebej uporabni kot dostavni sistemi učinkovin, v zdravstvu pa so možnosti njihove uporabe usmerjene predvsem v tkivno inženirstvo. Tkivno inženirstvo je mulitidisciplinarno področje, ki povezuje različne vede, predvsem kemijo, biologijo, materiale, medicino, farmacijo, biotehnologijo, itd. Je hitro razvijajoče se področje, ki je večinoma usmerjeno v možnosti regeneracije tkiv. Pri tem lahko uporabimo različne biomateriale, ki služijo kot tkivni nadomestek in pomagajo pri obnovi poškodovanega tkiva. Materiali, ki se uporabljajo za namene v tkivnem inženirstvu, morajo biti biokompatibilni. Obenem morajo imeti ustrezno hitrost biorazgradnje in netoksične produkte, ki imajo poznan metabolizem. Morajo imeti tudi ustrezne mehanske lastnosti (rigidnost podobno tkivom), obenem mora biti enostavna njihova izdelava.

Biorazgradljivi polimeri se razgradijo do biokompatibilnih in netoksičnih produtkov. Poznamo naravne in sintezne biorazgradljive polimere. Naravni biorazgradljivi polimeri vključujejo polisaharide, želatino, alginate, lipoproteine nizke gostote, serumske albumine, kolagen, itd. Poznano je, da omenjeni polimeri lahko povzročajo neželene učinke v telesu, zato je tudi omejena njihova uporaba. Poleg tega je zelo težavna njihova proizvodnja in postopek čiščenja. Zato so danes večinoma v uporabi sintezni biorazgradljivi polimeri, kamor vključujemo poliestre, polanhidride, polilaktone, poliaminokisline, polifosfoestre. Najbolj široko v uporabi je polimlečna kislina. Gre za alifatski poliester, ki je sintetiziran s polimerizacijo z odprtjem obroča cikličnih di-estrov mlečne kisline. Poznani so predvsem *D*-, *L*-, *DL*-, *LL*, in *DD*-polilaktid. Polimlečna kislina razgrajuje s hidrolitsko cepitvijo esterskih vezi. Pri tem kot stranski produkt nastane mlečna kislina, ki se v naslednji fazi razgradi do ogljikovega dioksida in vode.

Biorazgradljivi elastomeri so rahlo zamreženi polimeri, ki se lahko močno elastično deformirajo. Ponavadi imajo ti materiali temperaturo steklastega prehoda nižjo od telesne temperature. Še posebej zanimivi so elastomeri, ki so osnovani kot triblok kopolimeri polimlečne kisline in polietilenglikola. Polimlečna kislina je hidrofoben polimer z zelo počasno razgradnjo. Da povečamo hidrofilnost takega materiala, lahko v strukturo

polimera dodamo hidrofilne enote polietilenglikola. S spreminjanjem razmerja med enotami etilenoksida in laktidnimi enotami v strukturi polimera lahko vplivamo na kinetiko biorazgradnje takšnega polimera. Poleg ustreznega profila dekompozicije morajo takšni elastomeri izražati ustrezne mehanske lastnosti. Najosnovnejša metoda za merjenje mehanskih lastnosti materiala je natezni poskus. Pri tem poskusu vpet material raztegujemo na njegovih koncih. Beležimo silo, ki material raztegne za določeno dolžino. Na podlagi omenjenih parametrov lahko določimo natezno napetost (σ) in relativni raztezek (ε). Natezna napetost je definirana kot sila, ki se uporabi za raztegovanje vzorca, glede na začetno površino vzorca. Relativni raztezek je poznan kot razmerje med spremembo dolžine vzorca in začetno dolžino vzorca. Poznano je, da je elastična deformacija reverzibilna, tj. material se po deformaciji povrne v prvotno stanje. Elastično deformacijo ponavadi opredelimo z Youngovim modulom, ki opisuje Hookovo področje elastičnosti in je definiran kot razmerje med natezno napetostjo in relativnim raztezkom. Materiali z nižjim Youngovim modulom izražajo višjo elastičnost.

V magistrski nalogi smo sintetizirali različne biorazgradljive elastomere za uporabo v tkivnem inženirstvu. Kot začetni material smo uporabili že pripravljena triblok kopolimera polimlečne kisline in polietilenglikola (PLA-PEG-PLA) z različnima molekulskima masama ($TBCP_{4000}$ = 4000 g/mol in $TBCP_{12000}$ = 12000 g/mol) in različnim razmerjem med enotami etilenoksida in laktidnimi enotami. V naslednjem koraku smo izvedli reakcijo metakrilacije, pri čemer smo ustvarili dvojne vezi na koncu polimerne verige. Te vezi so nadaljnje uporabne pri kemijskem zamreževanju. Uspešnost reakcije metakrilacije smo ocenili na podlagi ^{1}H NMR-spektrov, pri čemer smo za kopolimer z višjo molekulsko maso določili 66% uspešnost metakriliranja. Pri kopolimerih z nižjo molekulsko maso smo ugotovili, da je reakcija metakriliranja potekla kvantitativno.

V drugem koraku smo pripravili različne elastomere (štiri za kopolimer višje molekulske mase in štiri za kopolimer nižje molekulske mase), pri čemer smo kot premreževalca uporabili dialildisulfid in pentaeritritoltetra-(3-merkaptopropionat). Obenem smo uporabili tudi različne foto-iniciatorje. Kemijsko zamreževanje smo izvedli pod UV-svetlobo in v nadaljevanju določili vsebnost gela ter temperaturo steklastega prehoda pripravljenih elastomerov. Pri vseh elastomerih smo ugotovili nižjo temperaturo steklastega prehoda od telesne temperature. Za elastomere nižje molekulske mase je bila temperaura steklastega

prehoda celo pod 0 °C. Obenem smo ugotovili tudi visoko vsebnost gela; in sicer njene vrednosti so bile za vse elastomere nad 90%.

V zadnjem delu smo izvedli mehanske teste (natezni test) in teste biorazgradnje. Natezni test smo izvedli v suhem in v mokrem stanju. Youngov modul smo določili iz naklona začetnega linearnega dela krivulje odvisnosti deformacije od obremenitve. Za izračun naklona krivulje smo uporabili linearno regresijo, pri čemer smo upoštevali, da je bil korelacijski koeficient večji kot 0,990. Ugotovili smo, da je bil Youngov modul višji za elastomere z nižjo molekulsko maso. Iz tega lahko sklepamo, da je imela molekulska masa večji vpliv na Youngov modul kakor dodatek premreževalca. Kljub temu je bil opazen vpliv premreževalca na Youngov modul pri elastomerih z nižjo molekulsko maso. Dialildisulfid, kot fleksibilna molekula, se lahko ureja med molekulami polimera tekom premreževanja, kar kaže na bolj kompaktno strukturo materiala in se odraža v višjem Youngovem modulu. Hkrati pa smo ugotovili tudi višjo natezno in zlomno trdnost ter relativni zlomni raztezek pri elastomerih z višjo molekulsko maso. S testom ANOVA smo pokazali, da hidratacija v večini primerov ni imela vpliva na elastičnost biofilmov.

S testi biorazgradnje smo dokazali, da je razgradnja v prvem mesecu testiranja v fosfatnem pufru počasna z zelo nizko izgubo mase. Po prvem mesecu je bila izguba mase zelo velika. Največja izguba mase je bila pri polimerih z nižjo molekulsko maso. Ugotovili smo, da na razgradnjo lahko vplivamo z razmerjem med enotami etilenoksida in laktidnimi enotami v stukturi polimera. Nasplošno, več kot imamo pristotnih hidrofilnih etilenoksidnih enot v strukturi, hitrejša bo razgradnja takšnega elastomera. Dokazali smo, da poleg omenjenega hidrofilnega/hidrofobnega razmerja enot v strukturi elastomera na biorazgradnjo vpliva tudi prisotnost hidrofilnega/hidrofobnega premreževalca. Ugotovili smo, da je biorazgradnja hitrejša, če imamo prisoten hidrofilen premreževalec (pentaeritritoltetra-(3-merkaptopropionat)).

Ključne besede: *tkivno inženirstvo, elastomer, Youngov modul, biorazgradnja, premreževalec*

THE LIST OF ABBREVIATIONS

DD – diallyl disulfide

DP – degree of polymerization

E – Young's modulus

ε_{break} – ultimate strain

E_{4000} – elastomers with molecular weight of 4000 g/mol

E_{12000} – elastomers with molecular weight of 12000 g/mol

EO/LA ratio – ratio of ethylene oxide and lactyl units

ECM – extra cellular matrix

ΔHm – melting enthalpy

M- TBCP$_{4000}$ – methacrylated triblock copolymer with molecular weight of 4000 g/mol

M- TBCP$_{12000}$ – methacrylated triblock copolymer with molecular weight of 12000 g/mol

Mn – number average molecular weight

PETMP – Pentaerythritol tetra(3-mercaptopropionate)

PEG – polyethylene glycol

PDI – polydispersity index

PLA – poly(lactic acid)

RSD – relative standard deviation

σ_{break} – ultimate stress

T_g – glass transition temperature

T_m – melting temperature

TBCP$_{4000}$ – triblock copolymer with molecular weight of 4000 g/mol

TBCP$_{12000}$ – triblock copolymer with molecular weight of 12000 g/mol

WL – weight loss

WU – water uptake

1 INTRODUCTION

1.1 TISSUE ENGINEERING AND TWO SPECIFIC STRATEGIES OF TISSUE ENGINEERING

Tissue engineering can be defined as an application of a different combination of cells, engineering, materials, methods and suitable biochemical factors for improvement or replacement of biological functions (1). The major purpose of tissue engineering is to design new scaffolds, to allow cells containment and regeneration of functional tissue in the host as an alternative to conventional organ transplantation and tissue reconstruction methods (1, 2). Tissue engineering scaffolds are three-dimensional supports for propagated cells and specific signalling molecules that imitate native tissue environments. The main aim of produced scaffolds is to provide temporary replacement of the damaged extracellular matrix (ECM), to immediately offer support for cell growth and accelerated tissue regeneration (4, 5). There are two specific types of tissue engineering strategies, cellular (»*in vitro*«) and acellular (»*in vivo*«) (4).

Cellular tissue engineering strategies are typically related to living host cells seeding and expanding into a scaffold in order to allow integration before implantation. The cells within scaffolds are then combined with the tissue to stimulate new tissue generation, while the scaffold material itself gradually degrades *in vivo* (2, 6, 7).

Direct implantation of an unseeded scaffold into an injured zone is common for acellular strategies. The main goals of such an approach are deposition of extracellular matrix (ECM) and associated structures to provide physical support for cells, as well as the biochemical signals required to encourage tissue morphogenesis, homeostasis and differentiation. Communication between cells and ECM is a dynamic and complex process in which various cellular responses are evoked by various chemical and physical characteristics of the ECM (2, 5 – 11).

1.1.1 BIOMATERIALS USED FOR TISSUE ENGINEERING APPLICATIONS

Biomaterials are defined as natural or synthetic substances able to interact with biological system and are usually divided into polymeric, ceramic and metallic types (2, 12). These materials support tissue function during intimate contact with it, externally as well as

internally. Biomaterials have been used in human or veterinary medicine to enable diagnosis or therapy (2). Development of new suitable biomaterials has always been a challenging topic of research which includes materials science, chemistry, biomedical science, biology, pathology, etc... Biodegradable polymers break down after their intended purpose to result in natural by-product. Those polymers are one of the most desirable materials in tissue engineering, due to their mechanical versatility and similarity to the structural tissue characteristics (2, 13, 14). It has been found that biodegradable polymers exhibit minimal long-term inflammation and complications related to the repeat surgical procedures, which makes them suitable for most medical applications (2, 15). A huge effort has been invested into the research and development of biodegradable polymers, which are able to mimic natural tissues (2, 16 – 18).

Ceramic biomaterials can be used for dental applications and orthopaedic implants. For orthopaedic implants, metallic biomaterials can also be used, they can be also used for cardiovascular applications (19, 20).

1.1.2 CLASSIFICATION OF BIODEGRADABLE POLYMERS FOR BIOMEDICAL AND TISSUE ENGINEERING APPLICATIONS

Biodegradable polymers can be classified according to their application, origin, chemical composition, synthesis method, processing method, mode of degradation, etc. For biomedical applications, biodegradable polymers, considering their origin, are classified as natural polymers, which are obtained from natural resources, and synthetic polymers. Both natural and synthetic polymers are utilized in a broad range of applications such as implantable, cardiovascular and transdermal as well as catheters (2, 21, 22).

Generally, polymers can be classified as thermoplastics, thermosetting polymers, elastomers and fibres. As a category of polymer biomaterials, biodegradable elastomers are one of the novel polymers used in soft tissue engineering. More about these materials will be described in the section 1.1.3. Based on the mode of degradation, polymeric materials are divided into enzymatically degradable polymers or hydrolytically degradable polymers. Enzymatic degradation is the most frequent for natural polymers (23, 24).

1.1.2.1 Naturally-occurring biodegradable polymers

Natural polymers are usually formed within cells by complex metabolic processes, including enzyme catalysed chain growth polymerization of activated monomers (22). Naturally-occurring polymers can be divided into the following three groups (25):

1. proteins (collagen, fibrin gels, etc.),
2. polysaccharides (chitosan, alginate, hyaluronic acid derivatives, etc.)
3. and polynucleotides (DNA and RNA).

Natural polymers as biomaterials exhibit several advantages, such as bioactivity and their chemical modification can have direct effect on their degradation. Due to positive biological recognition of their chemical make-up, natural polymers exhibit high degree of scaffold–tissue compatibility (25). Despite the fact that they can be considered as the first clinically used biomaterials, they also exhibit some undesirable properties such as a strong immunogenic response, due to impurities in material gained from processing and the possibility of disease transmission (23, 24, 25). Despite this, natural polymers can be used in a number of tissue engineering applications, including cardiovascular tissues and musculoskeletal tissues (26).

1.1.2.2 Synthetic biodegradable polymers

Synthetic biodegradable polymers offer a number of advantages when compared to natural ones. They have more predictable proprerties, are more easily reproducible and have a longer shelf life. The key advantages of these polymers include uniformity of microstructure, batch-to-batch uniformity and mechanical resistance with large-scale production. It is also known that synthetic biodegradable polymers are generally biologically inert and express degradation kinetics suitable for various applications. Furthermore, synthetic polymers can be designed with chemical functional groups that influence tissue in-growth (24, 25, 27). Polylactic acid, poly(caprolactone), (polyglycolic) acid, poly(glycolide) and poly[*d*,*l*-(lactide-co-glycolide)] have been widely used in tissue engineering due to their acceptable biocompatibility and excellent mechanical properties (28, 29). Other synthetic biodegradable polymers demonstrating large potential in tissue engineering are:

- polyanhydride (30),
- polyurethane (31, 32)
- polycarbonate (33, 34),
- poly(ester amide) (35),
- poly(amino acid) (36, 37) and
- poly-propylene fumarate (38).

Properties of the frequently used synthetic polymers in medicine are summarized in Table 1 (25).

Table I: The major synthetic biodegradable polymers used in medicine and their properties (25)

Polymer	**E (GPa)**	**Tm (°C)**	**Tg (°C)**	**Degradation products**	**Degradation time (months)**
Polylactic acid	2.7	173 – 178	60 – 65	*l*-lactic acid	12 – 18
Polyglycolic acid	7.0	225 – 230	35 – 40	Glycolic acid	3 – 4
Poly-lactic-co-glycolic acid	2.0	Amorphous	50 – 55	*d, l*- lactic acid and glycolic acid	3 – 6
Poly(propylene fumarate)	2 – 3	30 – 50	-60	Fumaric acid, propylene glycol and pol(acrylic acid-cofumaric acid)	> 24
Polyanhydride	-	50 – 90	-27	Carboxylic acids	0.14 – 1.4
Poly-phosphazene	-	-	-	Phosphate, ammonia, corresponding side groups	
Poly-(ε-caprolactone)	0.4	58 – 63	-60	Caproic acid	> 24

1.1.3 BIODEGRADABLE ELASTOMERS

Biodegradable elastomers can be defined as biodegradable elastic biomaterial used in human or veterinary medicine for targeted delivery of drugs (39). Their specific properties, such as their ability to provide a structural support for the regeneration of soft tissues (blood vessels and ligaments), to recover their shape after deformation and mechanical properties similar to native tissues in natural environment, display potential for a variety of applications. The main advantages of biodegradable elastomers are (24, 39, 40):

1. through chemical or physical cross-linking, an three-dimensional cross-linked network structure, similar to that of natural elastin can be attained;
2. extensive elasticity and flexibility;
3. comparable mechanical properties to soft body tissues;
4. biodegradability, directly controlled by crosslink density;
5. after the implantation in body, consequent surgical removal is not needed.

1.1.3.1 Classification of biodegradable cross-linked elastomers

Cross-linking is one of the main approaches for tailoring the mechanical properties of elastomers. Other physicochemical properties of biodegradable elastomers, influenced by cross-linking are (39, 41 – 43):

- melting point (T_m) and glass transition temperature (T_g);
- crystallinity;
- solubility and biodegradability;
- biocompatibility and bioactivity.

Physically cross-linked elastomers originate from hydrogen bonding or the presence of van der Waals forces. They are also called thermoplastic degradable elastomers and are generally linear A-B-A copolymers, synthesized by the polycondensation or by ring-opening polymerization. A and B in this structure are immiscible polymers, segregated in phase separated domains. One phase is amorphous with low T_g and can contribute to the flexibility and elasticity of the material. On the contrary, the other phase is a crystalline or high T_g region, which usually provides excellent strength and delays the biodegradation process (44). It has been reported that thermoplastic biodegradable elastomers based on the lactic acid and ε-caprolactone linear copolymers have Young's modulus (tensile modulus or modulus of elasticity) around 8 – 30 MPa and elongations at breaks (fracture strains) of more than 500% (46 – 48). Mechanical properties of these elastomers could be modified by combining different co-monomers, such as poly(ethylene glycol) (48 – 50), butandiol (51, 52) or butylene succinate (53). Thermoplastic degradable elastomers generally have great solvent and thermal processing properties and their crystallinity leads to the heterogeneous degradation. Consequently, the degradation rate is difficult to control and quite often induces a non-linear strength loss with time (39, 41).

Chemical cross-linking is usually irreversible and originates from the formation covalent bonds between polymer chains. Chemically cross-linked bio-elastomers are called thermoset elastomers and can be prepared from amorphous pre-polymers by polycondensation, ring-opening polymerization and microbial polymerization (39, 41, 44). It is known that these elastomers after solidifications are difficult to process into different shapes. Despite this disadvantage, thermoset elastomers are widely used for biomedical application due to the combination of bulk and surface erosion, which induces a linear loss of mechanical properties with degradation time. Thermoset elastomers also have high shape stability and tightly controlled network architecture (39, 54, 55). It has been reported that highly cross-linked polyester-amides (42, 44, 54, 56) and cross-linked co-polyesters based on ε-caprolactone, glycolic acid and lactic acid, express Young's modulus in the range 0.2 – 800 MPa and their elongation at breaking point is in the range 5 – 600% (57).

Photocured elastomers are one of class of thermoset elastomers. Photo-crosslinking compared to the thermo-crosslinking, enables easier control of material solidification *in vivo* and curing rate at room temperature with minimal heat production. Photo-crosslinking is also desirable because it minimizes cost of treatment, patient discomfort and risk of infection (39, 58, 59).

1.1.3.2 Polylactic acid

Polylactic acid (PLA, Figure 1) is a biodegradable thermoplastic aliphatic polyester, widely used for construction of cell scaffolds for tissue engineering purposes. The polymer exhibits excellent biocompatibility (60 – 62).

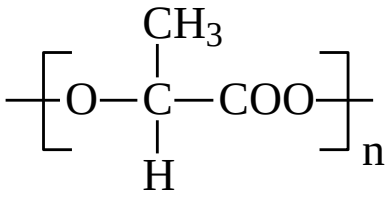

Figure 1: The structure of polylactic acid (PLA)

Lactic acid is present in three isomeric forms *l*-lactic acid, *d*-lactic acid and *d,l*-lactic acid. Pure *l*-lactic acid or *d*-lactic acid, or mixtures of both are used for the preparation of

polylactic acid (PLA), where four distinct materials can be produced: crystalline poly(*d*-lactic acid) (PDLA), hemi-crystalline poly(*l*-lactic acid) (PLLA), amorphous poly(*d,l*-lactic acid) (PDLLA) and *meso*-PLA. PDLA, PLLA and PDLLA degrade via hydrolysis of the ester bond even in the absence of a hydrolase (63). PLA is a very hydrophobic polymer, which provides much slower degradation with a half-life from 6 months up to 2 years. The degradation half-life depends on shape and size, isomer ratio and the temperature. Slow degradation makes it suitable for applications, where long-term mechanical integrity is highly desirable. The typical values of Young's modulus are around 3 GPa and 1.5 – 2.7 GPa for the tensile strength. Mechanical properties of PLA usually depend on its degree of crystallinity (25, 64, 65).

For synthesis of PLA, ring-opening polymerization (ROP) and direct poly-condensation are used as major synthetic methods. ROP (Figure 2) is the most effective method to produce high molecular weight PLA.

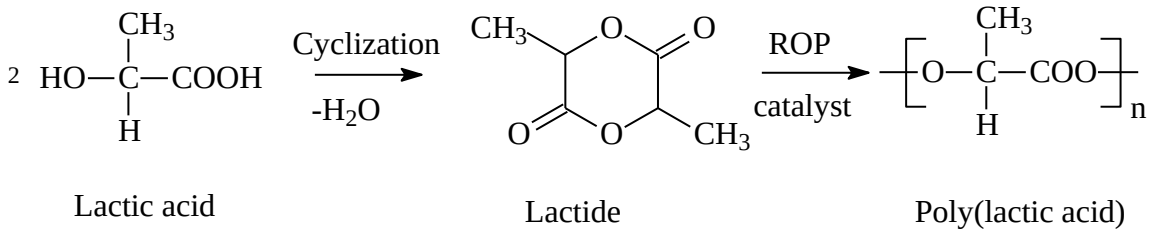

Figure 2: Synthesis of PLA by ring-opening polymerization (25)

The reaction is carried out under vacuum or an inert atmosphere for the dimerization of the lactic acid monomers. Usually high purity of the lactide monomers are required. Tin(II) 2-ethylhexanoate is the most widely used as a catalyst. It has been reported that heavy metal-based catalysts cause the contamination of the product making the purification of PLA difficult. Consequently, is very important to remove the metal contaminants before further applications. To avoid these problems, application of organocatalysts (4-(dimethylamino)pyridine (DMAP), N-heterocyclic carbene (NHC), thiourea-amine, etc.) could be valuable alternative (65, 66).

1.1.3.3 PLA-based biodegradable triblock copolymers for biomedical applications

When designing scaffolds, it is very important to achieve a sufficient number of seeded cells, which should be uniformly located throughout the entire scaffold. If a scaffold is mainly prepared from hydrophobic polymer, the cell suspension could be inhibited from penetrating into the pores of the scaffolds. (62, 67, 68). Very slow hydrolytic degradation rate, with less than 10% weight loss after 10 weeks has been observed for the PLA cross-linked co-polyesters (44, 69 – 71). To enhance hydrophilicity of PLA scaffold, the modification of the bulk properties of PLA could be used. This can be achieved by addition of poly(ethylene glycol) (PEG) into the PLA chains. The hydroxyl chain-end groups of PEG make it possible to copolymerize it with other monomers, for example by the ring-opening copolymerization of lactide. Besides hydrophilicity, PEG is known as an excellent biocompatible biomaterial, due to its non-toxicity and flexibility (65, 73). The incorporation of PEG makes the copolymer polar, which leads to increased hydrophilicity and consequently to the increased degradation rate. The elastomers, based on the poly(lactide)-poly(ethylene glycol)-poly(lactide), completely degrade within 8 – 9 weeks and are soft (44, 74, 75).

1.1.4 REQUIREMENTS FOR BIODEGRADABLE ELASTOMERS FOR TISSUE ENGINEERING APPLICATIONS

The tissue response to a biodegradable implant depends on multiple circumstances related to chemical, physical and biological properties of the material including the implant`s shape and the structure. The chemical, physical and mechanical properties of biodegradable material will vary during time and degradation products produced can have different levels of tissue (in)compatibility compared to the starting material. Biodegradable elastomers used for biomedical application should express the following important properties (24, 40):

1. acceptable shelf-life and degradation time; non-toxic degradation products, which are able to be metabolized and/or cleared from the body;
2. non-evoked sustained inflammatory or toxic response after the implantation;
3. appropriate mechanical properties for the indicated application; any variation in those properties should be compatible with the healing process;

4. appropriate permeability and processability for planned application;
5. biocompatibility;
6. bioactivity analogous to those of natural living substances and tissues.

Elastomers used for those applications usually have a glass transition temperature lower than body temperature. Furthermore, they express high elongation at break and completely reversible stress-strain curves (39, 76, 77).

1.1.5 BIODEGRADABILITY

Biodegradation of a polymer can be defined as cleavage of polymer chains caused by the hydrolysis reactions between molecular chain and water molecules. The water molecules react with the polymers chains and break their backbone (78). Naturally-occurring bio-elastomers are enzymatically degradable. Conversely synthetic biodegradable elastomers, which consist of hydrolytically labile anhydride, amide, ester and ortho-ester segments degrade hydrolytically (39, 79).

Biodegradation of elastomers depends on the following factors:

- chemical structure, molecular weight and its distribution;
- cross-linking bond type and cross-linking density;
- degree of crystallinity;
- porosity;
- hydrophilicity, hydrophobicity and
- biological conditions in the body.

It is generally expectable that faster degradation will occur for low molecular weight elastomers with low crystallinity, low crosslinking density, low T_g, strong hydrophilicity and high porosity (39, 80). Beside hydrolytic and enzymatic degradation, biodegradable elastomers also degrade via surface and/or bulk degradation (39, 81). Typical for surface degradation is that the material will start to degrade on the exterior surface. Bulk degradation occurs throughout the whole material equally (82). The latter occurs, if the degradation and weight loss of the specimen are closely correlated with the rate of water penetration into the specimen. In the initial phase, slow ingression of water into the material occurs. Because of that no significant difference in weight and molecular weight

is observed. After that, due to saturation, a decrease in molecular weight and a rapid increase in the degree of material hydration occurs. In the final step a significant and fast decrease in weight and molecular weight is noticeable. The bulk degradation of biodegradable elastomers is very advantageous for applications in soft tissue engineering (39, 83).

Surface degradation occurs when the degradation rate of a material is higher than the rate of water diffusion into the material. Degradation firstly happens on the surface of the material. The degrading specimen keeps its original shape and becomes thinner over time. For this reason, surface degradation is more predictable, consequently the surface degradation is desired for applications in controlled drug delivery (39, 81).

It has been reported, that poly-lactides mainly undergo hydrolytic degradation via bulk erosion. Degradation of the polymers starts with water uptake, followed by random fission of esters bonds and they degrade into lactic acid, which is a normal human metabolic product. During the degradation process, the number of carboxylic end-groups increases, which leads to a decrease in pH and autocatalytic degradation. Lactic acid breaks down into carbon dioxide and water (24). Poly-(*l*-lactide) is a slowly degrading polymer, with less than 10% weight loss after 10 weeks (24, 44). PEG hydrogels degrade via hydrolysis in a degradation process that does not require the presence of specific biological compounds, such as proteases. The degradation products are sufficiently low molecular weight (3.4-20 kDa) to allow clearance from the body (84).

1.2 MECHANICAL PROPERTIES AND TENSILE TESTING

The mechanical stability and well-matched mechanical properties to the host tissue are one of the most important requirements of biomaterials for their clinical application (2, 85). Tensile testing is a critical test, where the material is exposed to controlled tension until failure (86). Achieved parameters, obtained from tensile test, such as the ultimate strength, the yield strength, the elongation and the Young`s modulus are included in material specifications. The tensile testing proceeds by applying axial or longitudinal load at a specific extension rate to a specimen, with known dimensions. The stress and the strain are calculated from recorded load and extension rate (87).

1.2.1 TENSILE SPECIMENS

The typical tensile specimen is shown in Figure 3. Generally, the specimen has enlarged shoulders (ends) for stretching and a reduced gage section. To avoid any end effects from the shoulders, the gage section needs to be centered within the reduced sections. The total length of the reduced section has to be at least four times the diameter (86 – 88).

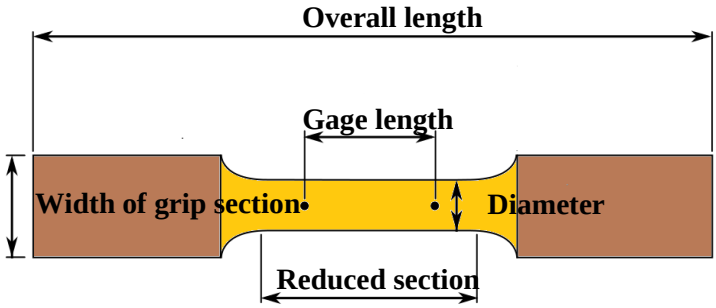

Figure 3: The typical specimen for tensile test

1.2.2 STRESS-STRAIN CURVES

A tensile test is carried out by stretching the specimen in a testing machine. The tensile force is recorded as a function of the increased gage length (86 – 88). The nominal stress (σ) can be defined as:

$$\sigma = \frac{F}{A_0} \qquad (1)$$

where F is the external tensile load and A_0 is the original cross-sectional area of the specimen. The strain (Equation 2), or also called nominal strain (ε) is defined as:

$$\varepsilon = \frac{L_f - L_0}{L_0} = \frac{\Delta L}{L_0} \qquad (2)$$

where L_0 is the original length of the specimen and L_f is the final length of the specimen. (86 – 88).

1.2.3 TYPES OF DEFORMATION

1.2.3.1 Elastic deformation

The elasticity of material refers to its ability to return to its original shape after the force was applied. When a material is exposed to a small initial stress, the bonds between atoms are stretched, because they move minimally from their equilibrium positions. Extensive alignment takes place in the neck (the cross-sectional area of the specimen, Figure3). The necking occurs, when the strain is irregularly localized in a small region of the material. In the range of elastic deformation, the stress is linearly proportional to the deformation. After removal of stress, the bonds relax and subsequently material returns to its original shape (Figure 4). Typical high elasticity of elastomers arises from their molecular structure and the distance between molecules within structure (89, 90).

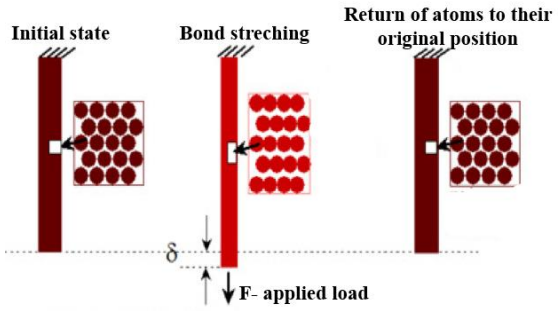

Figure 4: Elastic deformation (91)

The elasticity of material can be described by Hooke`s law (the stress is proportional to the strain), where the slope of initial linear region of stress-strain curve (Figure 6) is called the elastic modulus or Young`s modulus (E). E is a quantity used to measure a stiffness of an elastic material (90, 91).

E (Equation 3) is expressed as a ratio of a tensile stress σ (Pa) to the corresponding tensile strain ε (dimensionless).

$$\frac{F}{A} = E\,\frac{\Delta l}{l} \qquad (3)$$

The practical units used are mega-pascals (MPa or N/mm^2) or gigapascals (GPa or kN/mm^2) (92 – 94).

Polymers are often partially crystalline, where the crystalline regions are localized within the structure of the material. E for these materials is defined by the microstructure and by the elastic properties of crystalline and amorphous regions (95).

1.2.3.2 Plastic deformation and the fracture behavior

Under higher applied force, the yield stress (Figure 5) is exceeded and the tension overcomes the intermolecular forces. Consequently, stress-strain behavior will not be linear anymore and plastic deformation occurs. The point where the deformation starts to be non-linear is called the proportional (elastic) limit and indicates the onset of plastic deformation (Figure 6). This point is known as the yield point. Corresponding stress and elongation are noted as the yield strength (σ_{yield}) and elongation at yield (ε_{yield}). The yield stress can be calculated from the force at yielding, divided by the original cross-sectional area of the specimen (88, 89). If the force is continuously applied, the ultimate tensile strength (σ_{TS}) will be reached. The ultimate tensile strength is defined as maximum stress that a material can withstand before necking and breaking. The macroscopic deformation involves necking, where the neck is expanding along the specimen. The neck gets stiffer since deformation aligns the chains and increases local strength in the neck region (up to 2-5 times). In contrast to elastic deformation, material shape is not recovered after removal of applied force (Figure 6) (89, 90, 95).

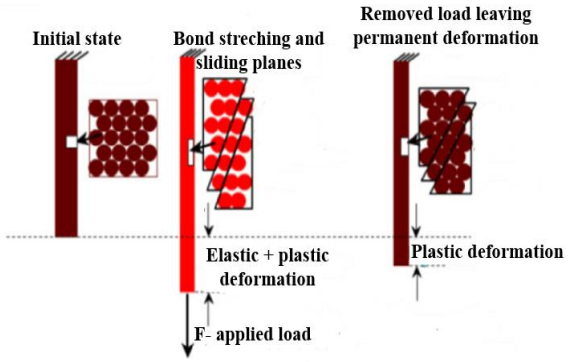

Figure 5: Plastic deformation (91)

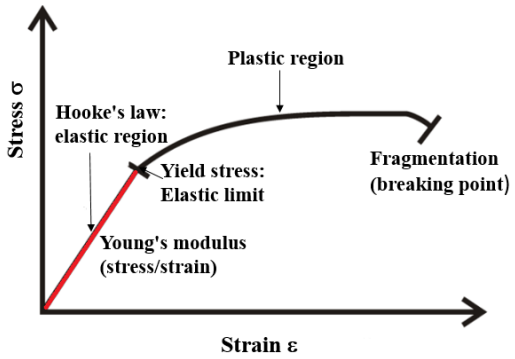

Figure 6: Typical stress-strain curve (91)

At the fracture point, the corresponding stress and strain are called the fracture strength and the elongation at break, respectively (Figure 6). The fracture strength is calculated by

dividing the force at fracture by the original cross-sectional area (88, 96). Regarding the tendency of a material to extend or fracture after the exceeded yield stress, materials can be classified as brittle and ductile (90). Brittle material will break sharply, without plastic deformation. On the other hand, ductile material will experience extensive plastic deformation before they fracture (90, 97).

2 OBJECTIVES OF THE STUDY

The main goal of this master thesis was the preparation of different biodegradable elastomers with desirable mechanical properties for biomedical applications, especially for soft tissue engineering (nasal cartilage and vascular vessels) and drug delivery. For this purpose, the thermoset degradable elastomers based on the photo cross-linking of poly(lactide)-poly(ethylene glycol)-poly(lactide) (PLA-PEG-PLA) triblock copolymers with different molecular weight were prepared.

In the first part of the experimental work, the methacrylation of PLA-PEG-PLA was carried out, where different molecular weights of PLA-PEG-PLA (Mn= 4000 g/mol and Mn= 12000 g/mol) were used as a starting material. The molecular weight of the triblock-copolymers were checked by size exclusion chromatography (SEC) and by ^{1}H NMR. The methacrylation efficiency was determined by ^{1}H NMR only.

In the second part of the research study, different elastomers were prepared by photo-cross-linking. Pentaerythritol tetra(3-mercaptopropionate) (PETMP) and diallyl disulfide (DD) were utilized as cross-linkers. Thermal properties (the glass transition temperature (T_g) and the melting point (T_m)), were determined by differential scanning calorimetry (DSC).

In the final phase, prepared elastomers were characterized with different physico-chemical methods. The study will be based on determination of mechanical properties and biodegradation. The E and other mechanical properties, including the ultimate tensile strength, ultimate strain and stress were determined by tensile strength testing in dry and hydrated state. The influence of the molecular weight and the cross-linker attributes on the mechanical properties was estimated. Statistically significant differences in mechanical properties of the elastomers in hydration state were determined using the statistical test ANOVA. In degradation tests, the weight loss and the water uptake after three months were evaluated. To simulate physical conditions, hydration tendencies of elastomers were tested in phosphate buffer solution (PBS), while elastomers based on the DD were additionally tested in solution of glutathione (GSH) and PBS. Impact of the amphiphilic balance of prepared triblock-copolymers, including the ratio of ethylene oxide and lactyl units, on degradation extent were examined, as well as the effect of the selected cross-linkers and their hydrophilic/hydrophobic character.

3 MATERIALS AND METHODS

3.1 MATERIALS

3.1.1 CHEMICALS AND BUFFERS

- ✓ Dihydroxy PEG (PEG_{45}, 2000 g/mol and PEG_{22}, 1000 g/mol), purchased from Sigma-Aldrich (St-Quentin Fallavier, France);
- ✓ tin(II) 2-ethylhexanoate (Sn(Oct)2, 95%), purchased from Sigma-Aldrich (St-Quentin Fallavier, France);
- ✓ trimethylamine (99%), purchased from Sigma-Aldrich (St-Quentin Fallavier, France);
- ✓ methacryloyl chloride (>97%), purchased from Sigma-Aldrich (St-Quentin Fallavier, France);
- ✓ diethyl ether, purchased from Sigma-Aldrich (St-Quentin Fallavier, France);
- ✓ dichloromethane, purchased from Sigma-Aldrich (St-Quentin Fallavier, France);
- ✓ acetone (≥99,5), purchased from Sigma-Aldrich (St-Quentin Fallavier, France);
- ✓ photo-initiator I651 (IRGACURE®651, 2,2-Dimethoxy-1,2-diphenylethan-1-one), purchased from Sigma-Aldrich (St-Quentin Fallavier, France);
- ✓ photo-initiator I184 (IRGACURE®184, 1-Hydroxy-cyclohexyl-phenyl-ketone), purchased from Sigma-Aldrich (St-Quentin Fallavier, France);
- ✓ cross-linker PETMP (Pentaerythritol Tetra(3-mercaptopropionat), purchased from Sigma-Aldrich (St-Quentin Fallavier, France);
- ✓ cross-linker diallyl disulphide, purchased from Sigma-Aldrich (St-Quentin Fallavier, France);
- ✓ *d,l*-lactide (*d,l-LA*), purchased from Purac (Lyon, France)
- ✓ PBS-phosphate buffer saline (10x pH 7.4), purchased from Invitrogen (Cergy Pontoise, France);
- ✓ glutathione (GSH, Mn = 421 g/mol) was kindly provided by IBMM

3.1.2 SMALL LABORATORY ACCESORIES

- ✓ Test tubes (10 ml, 25 ml, 100 ml);
- ✓ single use plastic pipettes and pipetting devices (Pipetman ultra produced by Gilson¸ Medibase);
- ✓ laboratory glassware (graduated cylinders, jars, Erlenmeyer flasks, beakers);
- ✓ syringe needles (BD);
- ✓ magnetic stirrer (Gilson);
- ✓ filters – yellow 0.45 μm (Ministar);

3.1.3 EQUIPMENT

- ✓ Size exclusion chromatography (SEC): VISCOTEK Malvern GPCmax, fitted with two Viscotek LT5000L mixed medium columns (300 × 7,8 mm) and VE 3580 RI detector; Worcestershire, UK;
- ✓ nuclear magnetic resonance spectroscopy (^{1}H NMR): AMX300 Bruker spectrometer (300 MHz); Billerica, Massachusetts, USA;
- ✓ differential scanning calorimetry (DSC): Perkin Elmer Instrument DSC 6000 thermal analyzer; Waltham, Massachusetts, USA;
- ✓ tensile tests: Instron 4444; Norwood, Massachusetts, USA;
- ✓ photo-cross-linking: UV light system DYMAX Light Curing System Model 2000 Flood; Torrington, Connecticut, USA;
- ✓ Advanced Chemistry Development (ACD/Labs) Software V11.02;
- ✓ Origin 9.0 software.

3.2 METHODS

3.2.1 PREPARATION OF PLA-PEG-PLA TRIBLOCK-COPOLYMERS

Custom made PLA-PEG-PLA triblock copolymers were already available and were used as a starting material. Firstly, prescribed amounts of *d,l*-lactic acid and PEG_{44} were placed into a flask, and then $Sn(Oct)_2$ (0,1 wt%) was added as catalyst. After degassing and sealing the flask under vacuum, the polymerization was carried out at 140 ˚C for 3 days. After the prescribed time, the copolymer was diluted in CH_2Cl_2 and precipitated in cold diethyl ether. Finally, the product was dried under reduced pressure to the constant mass.

For the calculation of polymerization degree of poly-lactic acid blocks ($\overline{DP}_{PLA}$) the following equation was used:

$$\overline{\boldsymbol{DP}}_{\boldsymbol{PLA}} = \frac{\mathbf{1}}{\mathbf{2}} \times \left(\frac{\overline{\boldsymbol{DP}}_{\boldsymbol{PEG}}}{\frac{\boldsymbol{EO}}{\boldsymbol{LA}}} \right) \qquad (4)$$

where $\overline{DP}_{PEG}$ is calculated considering the molecular weight of PEG provided by the supplier. EO/LA is the ratio of ethylene oxide and lactic units and was calculated from the integrations of protons of PLA blocks at 5.2 ppm and those of PEG blocks at 3.6 ppm (from the ^{1}H NMR spectra). The number average molecular weight ($\bar{M}_n$) of the synthesized copolymers was calculated as follows:

$$\overline{\boldsymbol{M_n}} = \mathbf{2} \times (\overline{\boldsymbol{DP}}_{\boldsymbol{PLA}} \times \mathbf{72}) + \overline{\boldsymbol{Mn}}_{\boldsymbol{PEG}} \qquad (5)$$

where 72 expresses the molecular weight of a lactic acid unit.

3.2.2 METHACRYLATION OF PLA-PEG-PLA TRI-BLOCK COPOLYMERS

PLA-PEG-PLA triblock copolymers were dissolved in freshly distilled CH_2Cl_2 (20% w/v) in three-necked flask. Triethlyamine (8 equivalents/chain) was then added under argon atmosphere and the solution was cooled down in an ice bath. After that, methacryloyl chloride (8 equivalents/ chain) was added from a dropping funnel and reaction was carried out in an oil bath at reflux for 66 h under stirring in the dark. After the prescribed time, the reaction medium was filtered repeatedly and the copolymer was precipitated in cold diethyl ether. All data for reactants used for methacrylation for M-$TBCP_{4000}$ are listed in Table 2 and for M-$TBCP_{12000}$ in Table 3. The precipitate was dissolved in acetone and later evaporated under vacuum. To check the presence of acetone and to calculate the

methacylation efficiency, NMR analyses were performed. Afterwards, methacrylated triblock copolymers were dried under reduced pressure to constant mass (for 24 h) stored in a cold and dark place.

Table II: Reactants, used for methacrylation of $TBCP_{12000}$

M-$TBCP_{12000}$			
Reactants	**$TBCP_{12000}$**	**Triethylamine**	**Methacryloyl chloride**
Weight (g)	22.84	5.81	6.48
n (mmol)	1.86	57.40	64.04
Equivalent	1.0	30.9	34.5
Molar mass (g/mol)	12300	101.19	101.19
Volume (ml)	/	8.00	6.00

Table III: Reactants, used for methacrylation of $TBCP_{4000}$

M-$TBCP_{4000}$			
Reactants	**TBCP4000**	**Triethylamine**	**Methacryloyl chloride**
Weight (g)	25.00	5.81	6.48
n (mmol)	7.58	57.40	61.99
Equivalent	1.0	7.6	8.2
Molar mass (g/mol)	3296	101.19	104.53
Volume (ml)	/	726	1080

Methacrylation efficiency was determined using the following equation:

$$\boldsymbol{Methacrylation\ efficiency} = \frac{\left(\frac{I_{5.7-6.1}}{2}\right)}{\left[\left(\frac{I_{5.7-6.1}}{2}\right)+\left(I_{4.3}-4\times\frac{I_{3.6}}{\overline{DP}_{PEG}\times 4}\right)\right]} \qquad (6)$$

where $I_{5.7-6.1}$ are integrations belonging to the alkenyl protons at 6.1 and 5.7 ppm. $I_{3.6}$ are integrations belonging to the PEG and non-methacrylated PLA chain ends at 4.3 ppm (45).

3.2.3 EVALUATION OF MOLECULAR WEIGHT AND POLYDISPERSITY BY SIZE EXCLUSION CHROMATOGRAPHY (SEC)

Size exclusion chromatography is a type of liquid chromatography in which separation mechanisms are based solely on the size of polymer molecules and in certain cases also on

the molecular weight of polymer in solution. It has become a standard technique for determinations of molar mass distribution and molar mass averages of polymers (97, 98).

A SEC instrument consists of (97, 98):

- a pump, which pushes the solvent through the system,
- an injector to enter the sample solution into the column,
- a column, where the separation happens,
- a detectors to detect the leaving components and
- an appropriate software for the calculation and demonstration of results.

The polymer sample is first dissolved in solvent to form a coil conformation. After that the sample is introduced into the mobile phase and allowed to flow into the column, filled with pored material (97, 98). When the dissolved polymer sample flows through the column, molecules larger than the biggest pores flow quickly, because they do not enter the pores and are carried with the mobile phase (97, 99). On the contrary, dissolved molecules smaller than the smallest pores, can penetrate into the pores and potentially occupy the stationary phase. Consequently, larger molecules take less time to exit the column, compared to the smaller molecules (100). Molecular weight distribution is made visible on the chromatogram and results from the pores sizes distribution.

Many polymers consist of a collection of molecules with various weights, which can results in differences in tensile strength, impact strength, hardness, etc. Average molecular weight includes number average molecular weight (M_n), weight average molecular weight (M_w), z-average molecular weight (M_z), and viscosity average molecular weight (M_v) (97, 98). The number average molecular mass (M_n) is the ordinary average of the molecular masses of individual macromolecules. Generally, this is a way of determining the molecular mass of a polymer. Polymer molecules, even the ones of the same type, come in different sizes (chain lengths for linear polymers), so the average molecular mass will depend on the method of averaging (101). It is calculated using the following equation:

$$\boldsymbol{M_n = \frac{\sum N_i M_i}{\sum N_i}} \qquad (7)$$

where the *Mi* is the molecular weight of the elution time and *Ni* is the number of molecules with particular molecular weight.

The weight average molecular weight (M_w), is another way for the description of the molar mass of a polymer. Some properties are dependent on molecular size, so a larger molecule will have a larger contribution than a smaller molecule. The mass average molar mass is calculated by the following equation (102):

$$\boldsymbol{M_w = \frac{\sum N_i M_i^2}{\sum N_i M_i}} \qquad (8)$$

It is known that the peak molecular weight in size exclusion chromatography varies between M_n and M_w (100, 101). The ratio between M_w and M_n is polydispersity index (PDI), which is used as a measure of width of molecular weight distribution for a particular polymer. PDI close to 1.0 means monodisperse polymer sample (100).

The number average molecular weights (M_n) and the polydispersity (PD) of the PLA-PEG-PLA triblock copolymers and then methacrylated triblock copolymers were estimated by using VISCOTEK GPCmax, fitted with two Viscotek LT5000L mixed medium columns (300 × 7.8 mm) and VE 3580 RI detector. Tetrahydrofuran (THF) was used as mobile phase at 1 ml/min flow rate and 30 ˚C. The polymer (5 mg) was dissolved in THF (1 ml). The solution was then filtered through 0.45 µm millipore filter before injection of 100 µl filtered solution. For calibration, polystyrene standards were used and according to them, *Mn* and *Mw* were depicted.

3.2.4 PREPARATION OF FILMS, PHOTO CROSS-LINKING AND GEL CONTENT (GC)

Defined amounts of PLA-PEG-PLA methacrylated triblock copolymers were dissolved in 5 ml of acetone under stirring. After that, the cross-linker was added (where prescribed). The photo-initiator was added eventually. Polymer solutions were degassed in ultrasonic bath for 10 min. The dissolved polymers were then decanted in silicon vessels and covered with perforated aluminum foil and shook under mild conditions for 15 minutes. The main purpose of shaking was to prevent the formation of bubbles. The prepared films were dried under reduced pressure for 30 min. The formulations are listed in Table IV.

Table IV: Elastomers formulations

Sample	Photo-initiator I184 (mol% / alkene)	Photo-initiator I651 (mol% / alkene)	PETMP (mol% /alkene)	AD (mol% / alkene)
$\mathbf{E_{12000\text{-}1}}$	10	0	0	0
$\mathbf{E_{12000\text{-}2}}$	0	10	25	0
$\mathbf{E_{12000\text{-}3}}$	0	10	0	25
$\mathbf{E_{12000\text{-}4}}$	5	5	12.5	12.5
$\mathbf{E_{4000\text{-}1}}$	10	0	0	0
$\mathbf{E_{4000\text{-}2}}$	0	10	25	0
$\mathbf{E_{4000\text{-}3}}$	0	10	0	25
$\mathbf{E_{4000\text{-}4}}$	5	5	12.5	12.5

To induce and enable cross-linking, the films, prepared by evaporation method, were exposed to UV light of DYMAX Light Curing System Model 2000 Flood for 15 min. Before soaking in CH_2Cl_2, the films were dried under reduced pressure for 2 hours. All unreacted prepolymers were fully extracted by soaking the films in CH_2Cl_2 for 24 hours. Eventually, the films were dried under reduced pressure for additional 24 hours. Gel content (GC) was calculated using the following equation:

$$\mathbf{GC} = \frac{\mathbf{m_{after\ extraction}}}{\mathbf{m_{before\ extraction}}} \times \mathbf{100}\% \qquad (9)$$

3.2.5 EVALUATION OF THERMAL PROPERTIES BY DIFFERENTIAL SCANNING CALORIMETRY (DSC)

DSC measurements were carried out under nitrogen (20 ml/min) Perkin Elmer Instrument DSC 6000 thermal analyzer (Waltham, Massachusetts, USA). The elastomer samples were analyzed under the following conditions: firstly, they were held for 1 min at 10 ˚C and in the second step they were heated from 10 ˚C to 110 ˚C at 5 ˚C/min. In the second cycle, the sample was cooled down to -60 ˚C with the rate of 10 ˚C/min and held under these conditions for 50 min. In the final cycle, the samples were heated from -60 ˚C to 200 ˚C with the rate of 5 ˚C/min. The T_g was determined on the last step (second heating ramp).

3.2.6 YOUNG´S MODULUS AND OTHER MECHANICAL PROPERTIES OF ELASTOMER`S

The elastomers were carefully cut into multiple specimens for tensile testing. The typical tensile specimens are shown in the Figure7. The dimensions of the specimens ($12 \times 2 \times 1$ mm^3) were held within the allowable tolerances established by the test procedure. The attachments areas at each end of the specimen were aligned with the axis of the bar.

Figure 7: Specimens for tensile tests

The electromechanical machine Instron 4444 (Norwood, Massachusetts, USA) was used as a testing equipment. For characterization in dry state, each elastomers specimen was analysed in triplicate at crosshead speed of 5 mm per min and at 37 ˚C. For analyses in hydrated state, the elastomers specimens were soaked in a phosphate buffer solution (PBS, pH 7.4) at room temperature for 1 h. After that, their mechanical properties in hydrated state were measured in water surroundings in the same manner as for dry state. Each specimen axis was properly aligned with the rolling direction. The specimen was placed in the machine grips, where the sufficient force capacity was used, so that they were not damaged during testing. The wedge grips inserts were contained within the cross-head, and the specimen tabs were fully engaged by the grips, as shown in Figure 8.

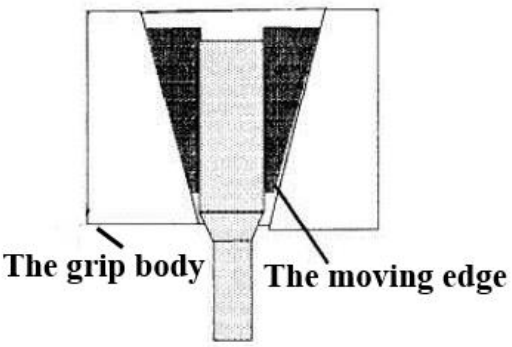

Figure 8: Proper engagement of a specimen in the wedge grips (89)

Each specimen was exposed to a stretching force, pulling at both ends of their length and was loaded until failure. Due to the preload of specimen, zero adjustment was not used. Instron 4444 software was used to acquire data for the applied stretching force (F) and for the change in gage length (Δl). Each change in gage length was calculated for applied cross-head speed. After that, stress-strain curves were plotted from sourced data. E (MPa), yield stress σ_{stress} (MPa), ultimate stress σ_{break} (MPa) and ultimate strain ε_{break} (%) were determined as the average of the three measurements and they were specified from plotted stress-strain curves, using Origin 9.0 software. Before the determination of mentioned values, each curve was smoothed in Origin 9.0, due to the huge capacity of sourced data and difficulty to determine the linear part on the stress-strain curves. For smoothing, Adjacent-Averaging was used as a method with 50 points of window for E_{12000} elastomers and with 15 points of window for E_{4000} elastomers. For the linear regression, the initial linear part, presented as range for Hook law, was determined in the range 55 – 180% for E_{12000} elastomers and around 5 – 40% for E_{4000} elastomers. The coefficient of determination was taken into account, which, for all samples, was more than 0,990. E was estimated by linear regression of slope of initial linear portion of smoothed stress-strain curve.

Ultimate stress σ_{break} and ultimate strain ε_{break} were determined as the last points of strain-stress curves before the fracture. The ultimate tensile strength was determined as the highest stress point in the plotted curves (Figure 9).

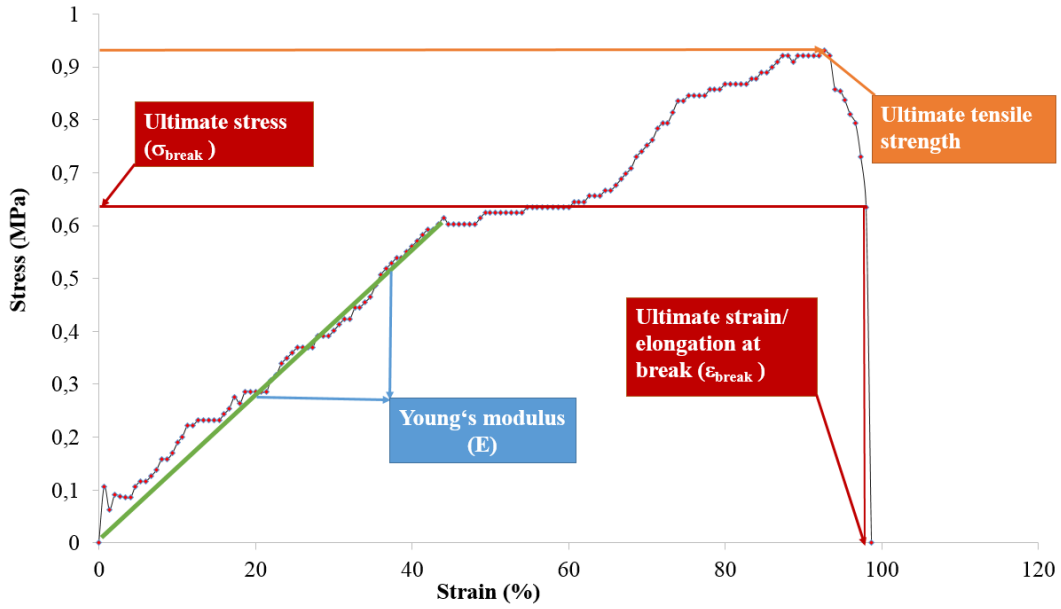

Figure 9: Graphical determination of Young's modulus, ultimate stress, ultimate tensile strength and ultimate strain

For the comparison of results in dry and in hydrated state, one way ANOVA with OriginPro 9.0 software was used, with the value 0.05 as a significance level.

3.2.7 DEGRADATION TESTS

Elastomer samples were cut, precisely weighed (initial dry weight of the sample before degradation, W_o) and placed in 5 ml of phosphate buffer solution (pH 7.4) at 37 ˚C under stirring. The analysis of each film was performed in triplicate during three months. At scheduled time points, the films were removed from PBS, gently dried on absorbent paper, and weighed (hydrated weight, W_h). After that, the samples were dried under reduced pressure at 40 ˚C for 24 hours and weighed again (dry weight of sample after defined period of time in PBS, W_d). The degradation was valuated using water uptake and weight loss. The water uptake (WU) and weight loss (WL) were calculated using the following equations:

$$\mathbf{WU} = \frac{(\mathbf{W_h} - \mathbf{W_d})}{\mathbf{W_d}} \times \mathbf{100} \qquad (10)$$

$$\mathbf{WL} = \frac{(\mathbf{W_0} - \mathbf{W_d})}{\mathbf{W_0}} \times \mathbf{100} \qquad (11)$$

Each result represents mean value of three replicates.

For degradation in glutathione (GSH) and PBS, elastomers consisting of DD as selected cross-linker were used. GSH is a small tri-peptide made up of glutamate (Glu), cysteine (Cys), and glycine (Gly). GSH plays important roles in the maintenance of intracellular redox state and as an antioxidant, cellular protectant and regulatory signalling molecule. It is a very important molecule in cell differentiation, proliferation and apoptosis. Any dysfunctions in GSH homeostasis or decrease in GSH/glutathione disulphide (GSSG) ratio leads to an increased susceptibility to oxidative stress and they are involved in the progression of many human diseases including cancer. On the other hand, cancer cells defend themselves from chemotherapy attack by hiking up their glutathione levels and they became more resistant to death, due to the elevated GSH levels (103 – 105). It has been reported that in the cytosol and nuclei, the concentration of GSH reaches 10 mM, while outside the cell the concentration is reduced to about 2–20 μM. In vivo studies on mice showed that in tumor tissues at least 4-fold higher concentrations of GSH were present in comparison to normal tissue (106 – 108).

At first, a 10 μM solution of GSH in PBS was prepared. After that, the elastomer specimens were weighed precisely and placed in 5 ml of the solution consisting of GSH and PBS at 37 ˚C under stirring.

4 RESULTS AND DISCUSSION

4.1 SYNTHESIS AND EVALUATION OF TRIBLOCK COPOLYMERS ($TBCP_{4000}$ AND $TBCP_{12000}$)

One of the main aims was to prepare biodegradable and biocompatible elastomers with sufficient mechanical robustness, related to shape recovery and elasticity. For this purpose, several films were prepared from triblock copolymers of PLA and PEG. Triblock copolymers (PLA-PEG-PLA) were synthesized by ring opening polymerization of *d,l*-lactic acid in the presence of PEG and $Sn(Oct)_2$ as selected catalyst. The formation of ABA-type triblock copolymers was achieved by using hydroxyl end groups of PEG, which has been used as macro-initiator for lactide polymerization (109).

Different block lengths of PLA-PEG-PLA triblock copolymers were reached by using different EO/LA ratios and different molecular weight of PEG. Two types of triblock copolymers were synthesized. The first type ($TBCP_{4000}$) was made from crystalline PEG_{45} (Mn = 2000 g/mol) and PLA_{50} with polymerization degree of 9 for each side and molar mass of 1300 g/mol. The second type of triblock copolymer ($TBCP_{12000}$) was prepared with PEG_{22} (Mn = 1000 g/mol) and PLA_{50} with polymerization degree of 78 for each side and molar mass of 11000 g/mol. PEG_{45} represented the hydrophilic block while amorphous PLA_{50} was used as a hydrophobic block. The mass yield for M-$TBCP_{4000}$ was about 90% and for M-$TBCP_{12000}$ was 67%.

The configuration, polymerization degree and molecular weight of synthesized triblock copolymers were evaluated with ^1H NMR spectroscopy. Typical NMR spectrum for $TBCP_{4000}$ is shown in Figure 10.

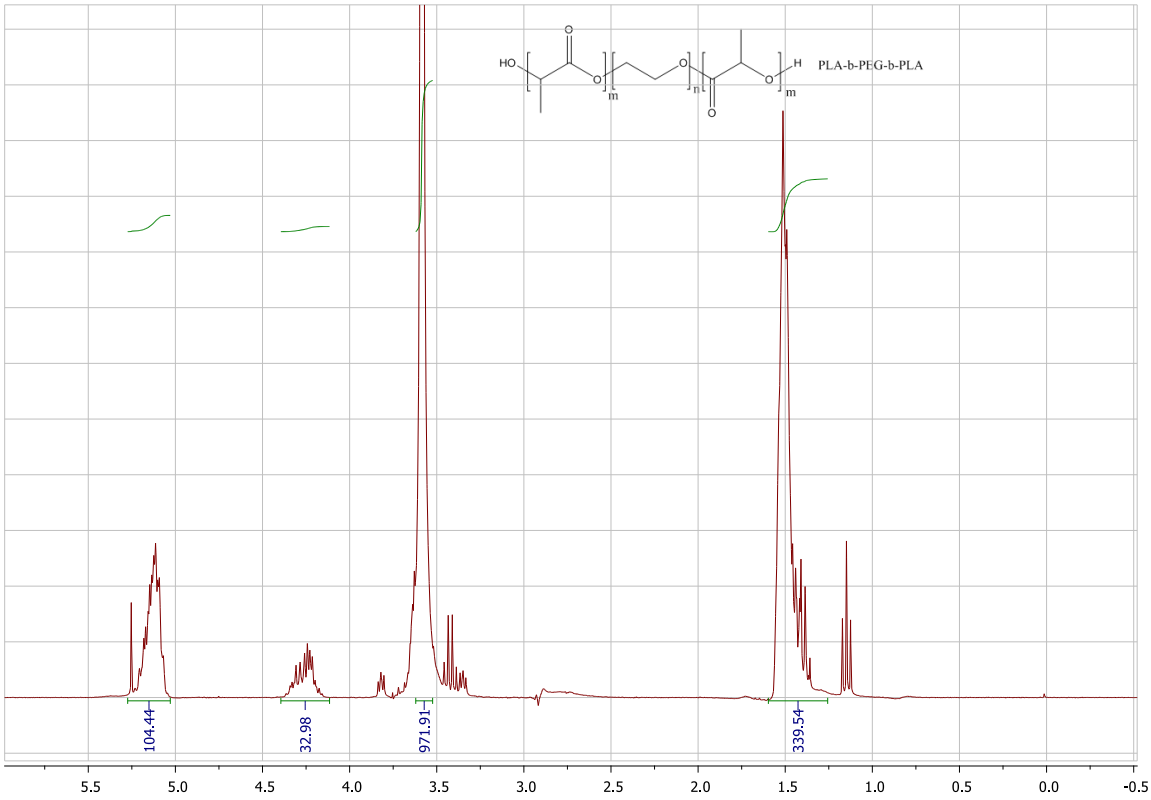

Figure 10: ^{1}H NMR spectra of synthesized triblock copolymer PLA-PEG-PLA

From the ^{1}H NMR spectra, the following peaks can be detected:

^{1}H NMR: (300MHz; $CDCl_3$): δ (ppm) = 5.2 (m, 1H, CO-CH(CH_3)-O), 4.3 (m, 1H, CO-CH(CH_3)-OH and 2H CH_2-CH_2-OH), 3.6 (s, 4H, CH_2-CH_2-O), 1.5 (m, 3H, CO-CH(CH_3)-O) (45).

The ratio of used ethylene oxide units and lactic units (EO/LA) in polymer structure can have an impact on the water solubility of this polymer and its degradation (110). When more hydrophilic ethylene oxide units (higher EO/LA ratio) are included in the polymer structure, better water solubility can be reached. Conversely, more lactic units (lower EO/LA ratio) in the polymer structure caused lower water solubility of this polymer. Additionally, lower molecular weight of PLA-PEG-PLA copolymers can induce improved solubility in water (110). EO/LA of synthesized triblock copolymers was specified as ratio of integrated protons of PEG blocks at 3.6 ppm and integrated protons of PLA blocks at 5.2 (44). The EO/LA ratio of prepared triblock copolymers was 2.4 for $TBCP_{4000}$ and 0.2 for $TBCP_{12000}$. Obtained results are comparable to literature data for polymers, which have

been used as a physical barrier to prevent the extent of tissue adhesions. The reported EO/LA ratio for those polymers was about 0.1 to about 100 (110).

Equation 5 was used for calculation of molecular weight (Mn) of the synthesized triblock copolymers and determined values were 12100 g/mol for $TBCP_{12000}$ and 3300 g/mol for $TBCP_{4000}$.

Table V: The comparison of mass yield, Mn, DP, PDI and EO/LA ratio for triblock copolymers before methacrylation

	M-TBCP $_{12000}$	**M-TBCP $_{4000}$**
Mass yield (%)	67	90
Mn (NMR) (g/mol)	12300	3300
Calculated (NMR) DP for each PLA side chain	78	9
Mn (SEC) (g/mol)	9000	4700
PDI	1.54	1.10
EO/LA ratio	2.4	0.2

Compared to the SEC analyses, the molecular weight (Mn) values were varied for 1000 g/mol or even more than those, calculated by NMR. The difference could be explained by the amphiphilic nature of copolymers (44). Once the polymer is dissolved, molecules form a coil conformation. While being analysed with SEC, dissolved polymer molecules start to behave like tiny spheres and their size depend on the molecular weight. The amphiphilic nature of polymer can have an effect on coil conformation. Therefore, the hydrodynamic volume can be modified and retention time will increase in the case of amphiphilic polymers (44, 111). SEC chromatograms of analysed polymers were monomodal, indicating that no homopolymer PLA was formed. PDI was 1.1 for $TBCP_{4000}$ and about 1.5 for $TBCP_{12000}$, which represented narrow distribution. Typical SEC chromatogram for $TBCP_{12000}$ is shown in Figure 11.

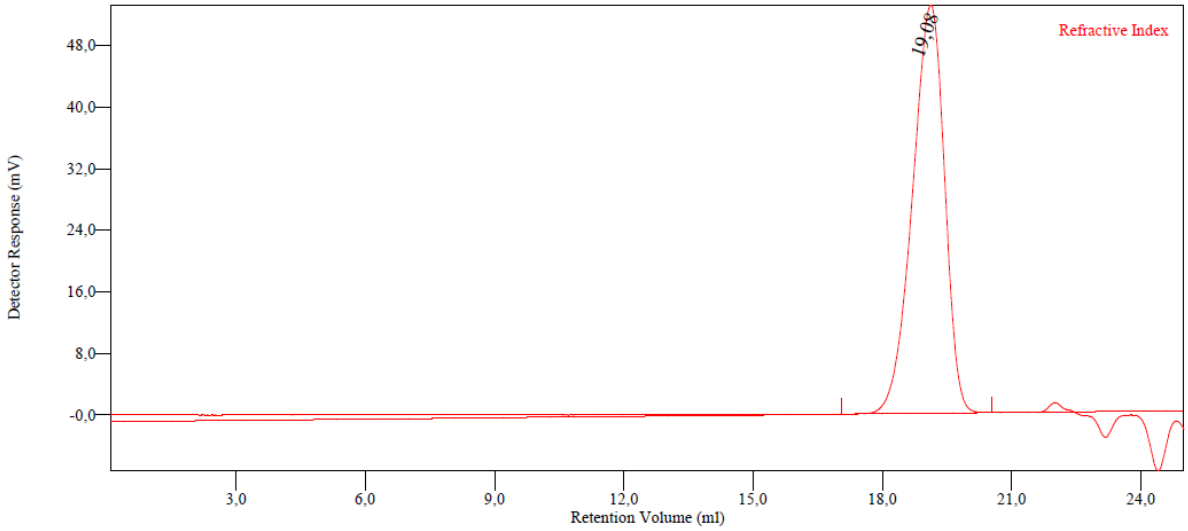

Figure 11: SEC chromatogram for $TBCP_{1200}$

4.2 METHACRYLATION OF TRIBLOCK COPOLYMERS (M-$TBCP_{4000}$ AND M-$TBCP_{12000}$)

Photo-cross-linkable triblock copolymers were prepared by methacrylation of PLA-PEG-PLA copolymers (Table V). Methacryloyl chloride was used as a methacrylation agent. The reaction of the end hydroxyl groups of triblock copolymers with methacryloyl chloride in the presence of triethylamine was utilized to prepare photo-reactive vinyl groups. During the reaction the main side-product was hydrochloric acid. To neutralise the acid, the prescribed amount of tri-ethylamine was added in the dissolved copolymer. Mass yield of the reaction was 93% for M-$TBCP_{12000}$ and 67% for M-$TBCP_{4000.}$ Methacrylation efficiency was calculated from the integrations of protons belonging to the alkenyl groups at 5.7 ppm and 6.1 ppm and that of non-methacrylated PLA and PEG end groups at 4.3 ppm (44). The values were equal to 66% for $TBCP_{12000}$ and more than 100% for $TBCP_{4000}$, which means that the reaction was completed. For $TBCP_{12000}$, lower methacrylation efficiency is attributed to the sterical hindrance that makes the chain-ends less accessible for reaction. It was assumed that high efficiency of methacrylation for M-$TBCP_{4000}$ could also be attributed to the enlargement of NMR spectra. Such an enlargement had to be done for the calculation of efficiency and also caused increase of integrals. The increase of the integrals therefore caused efficiency over 100%. SEC analyses were used, where chromatograms peaks were mono-modal with PDI 1.09 for M-$TBCP_{4000}$ and 1.36 for M-$TBCP_{12000}$. The comparison of triblock copolymers

properties after methacrylation is presented in Table VI. A slight decrease in molecular weight of M-TBCP$_{12000}$ and in the difference in polymerization degree for M-TBCP$_{4000}$ before and after methacrylation were observed due to the modification of the amphiphilic character of the block copolymer (44).

The thermal properties for M-TBCP$_{4000}$ were determined by DSC (Table VI). Based on the present T_m and T_g, M-TBCP$_{4000}$ can be considered as semi-crystalline.

Table VI: The comparison of mass yield, methacrylation efficiency, Mn, DP, PDI and EO/LA ratio for copolymers and their thermal properties after methacrylation

	M-TBCP $_{12000}$	**M-TBCP $_{4000}$**
Mass yield (%)	92.7	60.6
Methacrylation efficiency (%)	66	115
M_n (NMR) (g/mol)	12280	3600
Calculated (NMR) DP for each PLA side chain	78	10
M_n (SEC) (g/mol)	11800	5700
PDI	1.36	1.10
EO/LA ratio	2.4	0.2
T_g (˚C)	-	15
T_m (˚C)	-	29
ΔH_m (J/g)	-	62

4.3 PREPARATION OF ELASTOMERS AND THEIR EVALUATION

Eight films (four from M-TBCP$_{4000}$ and four from M-TBCP$_{12000}$) were prepared with different formulations, where PETMP and DD were used as selected cross-linkers. Preparations were varied by the utilization of different cross-linkers and photo-initiators as well as their different concentrations. The simplest formulations (E$_{4000\text{-}1}$ and E$_{12000\text{-}1}$) were based on the addition of prescribed amount of IRGACURE® 184, as the selected photo-initiator. Other elastomers were prepared from different cross-linkers and photo-initiators with respect to the alkene groups in the structure of copolymers. E$_{12000}$ elastomers, made from M-TBCP$_{12000,}$ were slightly orange and transparent. On the other hand, E$_{4000}$ elastomers (made from M-TBCP$_{4000}$) had rough and uneven surface with the small PLA-enriched regions presented in the centre of the elastomers. The presence of these PLA-enriched regions could be attributed to the initial inhomogeneous evaporation of the solvent. It was assumed that the solvent began to evaporate at the edges of the silicon

vessels, which caused the concentration of PLA to slowly increase above its solubility and lead to the formation of particles.

After the UV cross-linking, all unreacted pre-polymers were removed from elastomers by soaking in CH_2Cl_2 for 24 hours. Gel content (GC) was evaluated after drying. The GC values were in the range 92 – 97%, which is higher, compared to previous published results, where typical gel content was about 74% to about 81% (45). The calculated values for GC are listed in Table VII. Slightly higher gel content, for about 2 – 5%, was estimated for E_{12000} elastomers, compared to the E_{4000} elastomers. The highest GC value was found for elastomers without added cross-linkers ($E_{12000\text{-}1}$ and $E_{4000\text{-}1}$). For E_{4000} elastomers, a slight decrease in GC values was observed within formulations, where the lowest GC value was found for $E_{4000\text{-}4}$ elastomer, prepared as a combination of PETMP and DD.

Table VII: Elastomers GC and thermal properties

Sample name	GC (%)	T_g (˚C)	T_m (˚C)	$_{\Delta}H_m$ (J/g)
E_{12000}-1	97,4	19,0	-	-
E_{12000}-2	96,8	18,3	-	-
E_{12000}-3	95,9	14,8	-	-
E_{12000} -4	96,4	20,8	-	-
E_{4000}-1	95,8	-46,3	26,2	12,9
E_{4000}-2	94,8	-41,9	22,0	5,3
E_{4000}-3	93,4	-44,6	21,0	10,1
E_{4000}-4	91,9	-41,12	-	-

E_{12000} elastomers had much higher T_g compared to the lower molecular weight elastomers, where T_g were below 0 ˚C. As expected, T_g increased, but only slightly, with the presence of cross-linker for elastomers with lower molecular weight. This was not the case with E_{12000} elastomers, probably due to the influence of the PLA segments and the restriction of chains mobility. All results are in agreement with the loose network, expected for long (12000 g/mol) pre-polymer chains. As expected, T_g was lower, when DD was used as cross-linker instead of PETMP. It was assumed that the difference could be attributed to the fact that DD can form only two bonds with the elastomer, while PETMP can form four bonds (the structures of cross-linkers are drawn in Figure 12). For that reason, a more compact cross-linked structure is expected for PETMP. Therefore the T_g was higher.

Based on results from Table VII, all values of T_g were below body temperature, which can contribute to the appropriate mechanical properties of material under physiological conditions. The melting enthalpies (ΔH_m) were low. No T_m was detectable for E_{12000}. Consequently E_{12000} elastomers could be considered as amorphous. Detailed confirmation of their amorphous structure should be in further determined with other experimental techniques.

4.4 MECHANICAL PROPERTIES OF ELASTOMERS

The major purpose of biomaterial's application is to mimic native tissue, so they potentially play an important role as an artificial extracellular matrix to support tissue regeneration (44). For this reason, we were interested in the evaluation of dependence between molecular weight of used copolymer and cross-linker nature and mechanical behaviour. Based on structural properties, higher stretching inside the structure and consequently higher elasticity was expected for elastomers produced with DD as cross-linker in comparison to those where PETMP was used. Due to the S-S bonds included in the molecular composition and consequently less sterical repulsion, higher elasticity was expected. Mechanical properties have been estimated from the strain-stress curves. The E (MPa), the ultimate strain ε_{break} (%), the ultimate tensile strength (MPa) and their relative standard deviations values RSD (%) are summarized in Tables VIII and IX.

Table VIII: Elastomers' mechanical properties in the dry state at 37 °C (Young's modulus (E), ultimate stress (σ_{break}), ultimate strain (ε_{break}), the ultimate tensile strength and their relative standard deviations (RSD))

Sample	E (MPa)	E_{RSD} (%)	σ_{break} (MPa)	σ_{break} RSD (%)	ε_{break} (%)	ε_{break} RSD (%)	Ultimate tensile strength (MPa)
$E_{12000\text{-}1}$	0.7 ± 0.1	15.2	1.6 ± 0.7	45.7	200 ± 49	24.5	1.7 ± 0.7
$E_{12000\text{-}2}$	0.5 ± 0.1	15.1	1.8 ± 0.6	30.6	314 ± 25	25.5	1.8 ± 0.6
$E_{12000\text{-}3}$	0.5 ± 0.1	27.5	1.1 ± 0.2	16.1	192 ± 1	0.6	1.2 ± 0.1
$E_{12000\text{-}4}$	0.7 ± 0.3	40.3	2.3 ± 0.6	25.0	242 ± 9	3.6	2.5 ± 0.8
$E_{4000\text{-}1}$	2.2 ± 0.3	12.7	0.7 ± 0.1	6.9	25 ± 2	7.8	0.8 ± 0.1
$E_{4000\text{-}2}$	1.6 ± 0.1	3.2	0.9 ± 0.1	4.6	45 ± 1	2.5	0.9 ± 0.1
$E_{4000\text{-}3}$	2.5 ± 0.7	27.6	0.7 ± 0.3	38.9	15 ± 5	33.3	0.7 ± 0.3
$E_{4000\text{-}4}$	1.6 ± 0.1	4.3	0.6 ± 0.1	12.5	29 ± 3	11.1	0.6 ± 0.1

Table IX: Elastomers' mechanical properties in the hydrated state at 37 °C (Young's modulus (E), ultimate stress (σ_{break}), ultimate strain (ε_{break}), the ultimate tensile strength and their relative standard deviations (RSD))

Sample	E (MPa)	E_{RSD} (%)	σ_{break} (MPa)	σ_{break} RSD (%)	ε_{break} (%)	ε_{break} RSD (%)	Ultimate tensile strength (MPa)
$E_{12000\text{-}1}$	1.1 ± 0.3	23.8	2.9 ± 0.2	7.7	292 ± 36	12.4	4.1 ± 0.8
$E_{12000\text{-}2}$	0.8 ± 0.1	5.3	2.1 ± 0.5	23.3	341 ± 42	12.3	2.1 ± 0.5
$E_{12000\text{-}3}$	0.6 ± 0.1	23.6	1.5 ± 0.4	30.4	181 ± 13	7.5	1.5 ± 0.4
$E_{12000\text{-}4}$	0.8 ± 0.2	19.4	2.6 ± 0.8	30.9	301 ± 34	34.5	2.7 ± 0.9
$E_{4000\text{-}1}$	1.5 ± 0.2	11.1	0.27 ± 0.01	3.70	21 ± 18	12.4	0.3 ± 0.1
$E_{4000\text{-}2}$	1.3 ± 0.4	31.1	0.44 ± 0.01	2.55	21 ± 6	12.3	0.44 ± 0.01
$E_{4000\text{-}3}$	1.9 ± 0.6	30.0	0.5 ± 0.1	15.7	15 ± 10	7.5	0.59 ± 0.03
$E_{4000\text{-}4}$	1.4 ± 0.2	13.3	0.3 ± 0.1	19.9	11 ± 4	20.8	0.3 ± 0.1

The values of determined E ranged from 0.44 to 2.46 MPa, which is lower compared to the published results, where values were around 2.2 – 4.5 for elastomers, consisting of 2,4,6-triallyloxy-1,3,5-triazine (TAC) and penta-erythitol triallyl ether (PETAE) as chosen cross-linkers (44). The simplest elastomer without cross-linker had E of 0.7 MPa for $E_{12000\text{-}1}$ and 2.2 MPa for $E_{4000\text{-}1}$. The latter value is comparable to the literature data, where E for PLA-PEG-PLA based elastomers with similar molecular weight, was also around 2.2 MPa (44). As expected, molecular weight had significant effect on E, when compared to the cross-linker nature. In dry state, E_{12000} elastomers possessed higher elasticity in comparison to E_{4000}. Longer chains in E_{12000} elastomers expressed higher degree of bending, which made it possible for them to be more flexible and the possibility of existence in large variety of available random configurations (44). Under an applied load, those chains are straightened and more lengthened, compared to the short one. These elastomers presumably were more amorphous, which means less ordered structure, compared to the shorter polymer chains in E_{4000} elastomers.

As mentioned previously, E_{4000} elastomers were rough and corrugated on the surface and with small regions of phase separation (visible crystallization) presented in the centrum of each elastomer. When exposed to the deformational stress, they fractured more easily explaining their brittle character. Mainly, E_{4000} tensile specimens were thinner. Due to the thin cross-sectional area and shorter chains of these elastomers, molecules were packed more densely within structure. Consequently, more rigid structure with higher E was determined. $E_{4000\text{-}2}$ elastomer, prepared with PETMP had lower E compared to the $E_{4000\text{-}3,}$ prepared with DD. Explanation could be attributed to molecular structure of the

cross-linker. Molecule of PETMP is large and inflexible, therefore due to the sterical repulsion dense structure of the film cannot be attained. As mentioned previously, DD can form only two bonds with each elastomer, while PETMP can form four bonds (Figure 12 A). As a consequence, higher elasticity is achieved for PETMP based elastomers, when compared to DD based elastomers. DD molecule is smaller and flexible (less sterical hindrance can be expected) and allowed dense packing of cross-linkers chains within polymer molecules. No significant difference in E was observed for of $E_{12000\text{-}2}$ and $E_{12000\text{-}3}$.

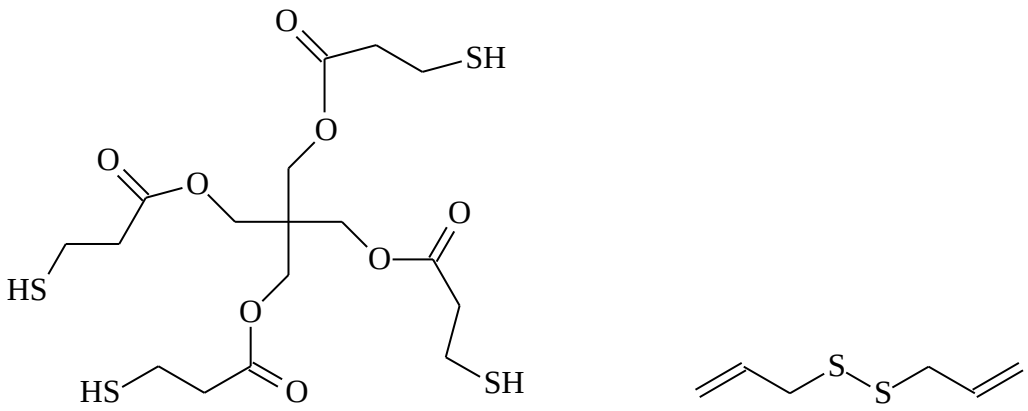

Figure 12: Chemical structure of PETMP (A) and DD (B)

Higher ultimate stress, strain and strength were noted for E_{12000} biofilms, where the highest ultimate tensile strength was observed in case of $E_{12000\text{-}4}$. For E_{4000} elastomers, less energy for break was needed, where the values for ultimate tensile strength and for ultimate stress were below 1 MPa.

It was assumed that the reasons for higher ultimate tensile strength of the E_{12000} elastomers could be related to the amorphous structure of those elastomers. It was suspected that amorphous polymer chains became more tightly packed while a higher load was applied. So during tensile test, first a higher load had to be applied to overcome elastic and plastic deformations until a fracture was reached. Presumably E_{12000} elastomers had longer chains that were more tangled. Therefore more chains had to be broken to achieve overall fracture in elastomer structure (78). Those reason could be the cause for higher ultimate tensile strength and ultimate strain. For all E_{12000} specimens necking was conspicuous during tensile testing.

On the other hand, crystal regions in E_{4000} elastomers were presumably more rigid and therefore broke more easily, compared to the E_{12000} elastomers. Also those elastomers were speculated to have shorter chains and were therefore less entangled. So due to the shorter chains, less (chain) points of breakage existed. Shorter chains were also presumably less elastic. Therefore a lower load had to be applied to achieve the tensile strength and the elongation at break (78).

Slight influence on the elongation at break was also established and related to the cross-linker's type. The most deformable were PETMP based elastomers while DD-based bio-films expressed lower elongation at breaks.

Elastomers hydration was carried out in PBS for 1 hour and their effects were non-significant on the E. However, some changes were noticeable in two samples. Exposure of samples in PBS leads to the swelling of material. It has been published that elastomers with similar properties have the highest swelling degree if they were prepared without cross-linkers (44). The decrease in swelling was found with the increment of cross-linker concentration. Moreover, choice of cross-linker and the balance between hydrophilic and hydrophobic segments had a significant influence on swelling (44).

Statistical analyses with ANOVA demonstrated no significant change between E of specimens in dry and in hydrated state. Only for $E_{4000\text{-}1}$ and $E_{12000\text{-}2}$, significant difference was noticeable in hydrated state. Interestingly, the hydration had more effect on the ultimate strain, the ultimate tensile strength (Table IX). Generally, E_{12000} elastomers expressed higher ultimate strain, the ultimate tensile strength and the ultimate stress in the hydrated state. That could be attributed to the reduced entanglement of long polymer chains, during the soaking in PBS solution. When long polymer chains were exposed to the tensile load, it was assumed that they started to unravel, rather than broke. Consequently more energy for deformation was utilized, which resulted in higher values of elongation at break, ultimate tensile strength and ultimate stress (78).

When E_{4000} elastomers were exposed in PBS solution, they swelled. Due to shorter chains and higher EO/LA ratio (2.4), water efficiently penetrated inside the structure of film and certain shorter chains started to unfold. Consequently, less energy was needed for deformation, which resulted in lower ultimate tensile strength, elongation at break and ultimate stress.

Determined mechanical properties are in the range of results from literature for soft natural tissues as vascular vessels (E = 1 MPa, ε_{break} =100%) and myocardium (E = 0.1 – 0.5, ε_{break} >20%) (79).

4.5 DEGRADATION PROFILE FOR ELASTOMERS IN PBS

In prepared elastomers, incorporated ester chains are capable of hydrolytic degradation. As mentioned previously, elastomers degrade via surface degradation (or surface erosion), bulk degradation (or bulk erosion) or a combination of both (39, 81).

Elastomers degradation was estimated by weight loss evaluation of prepared films. Each sample was soaked in PBS at 37 ˚C during three months. The weight loss and the water uptake were estimated at prescribed time points by weighing elastomers samples before and after degradation. The weight loss and the water uptake during prescribed time are shown in Figures 13 – 16. The selected cross-linkers, PETMP and DD had great differences in their solubility. PETMP (logP = 2.8 ± 0.4) is more hydrophilic than DD (logP = 3.5 ± 0.2).

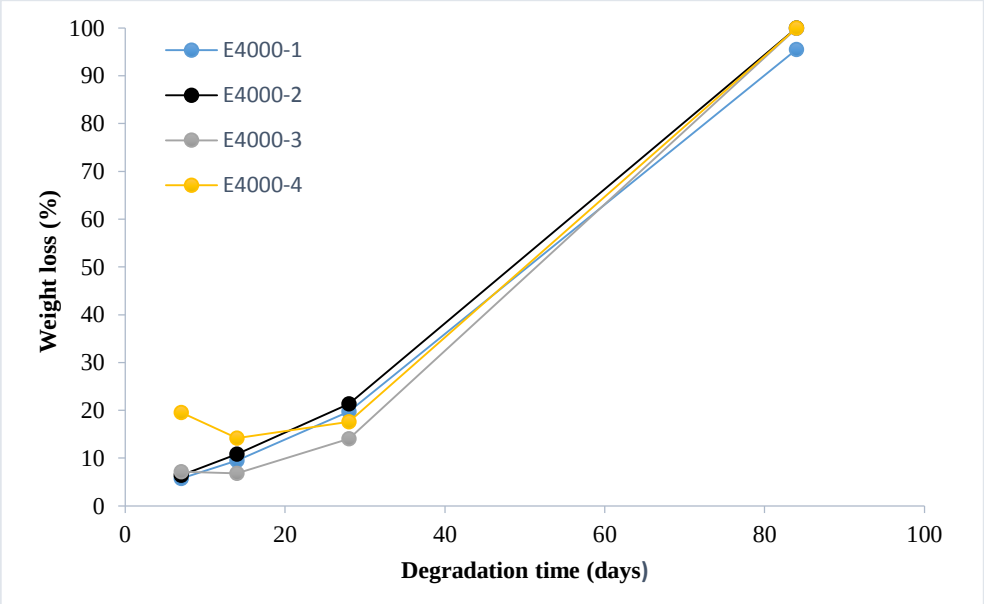

Figure 13: The weight loss for E_{4000} elastomers

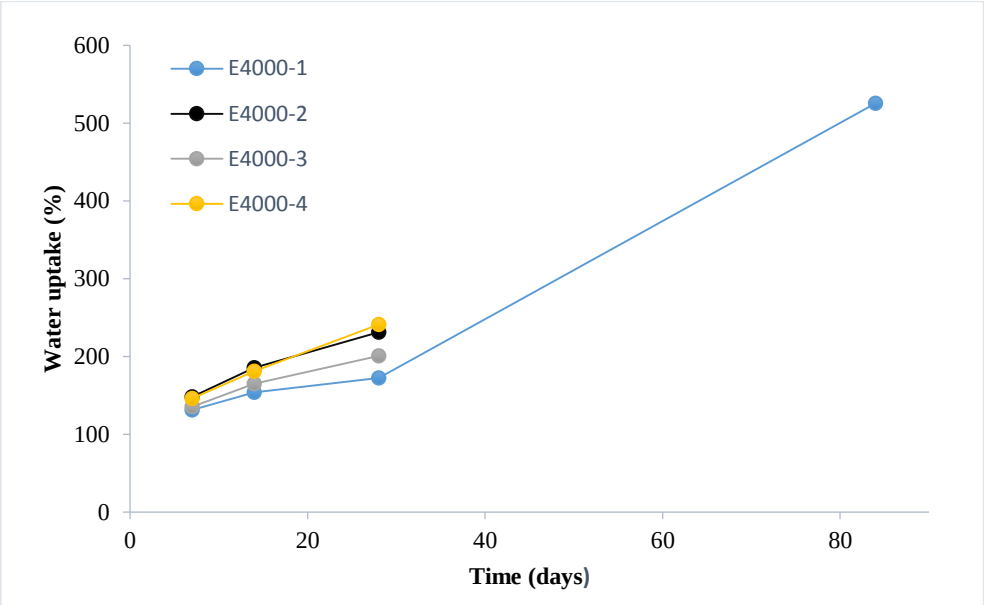

Figure 14: The water uptake for E_{4000} elastomers

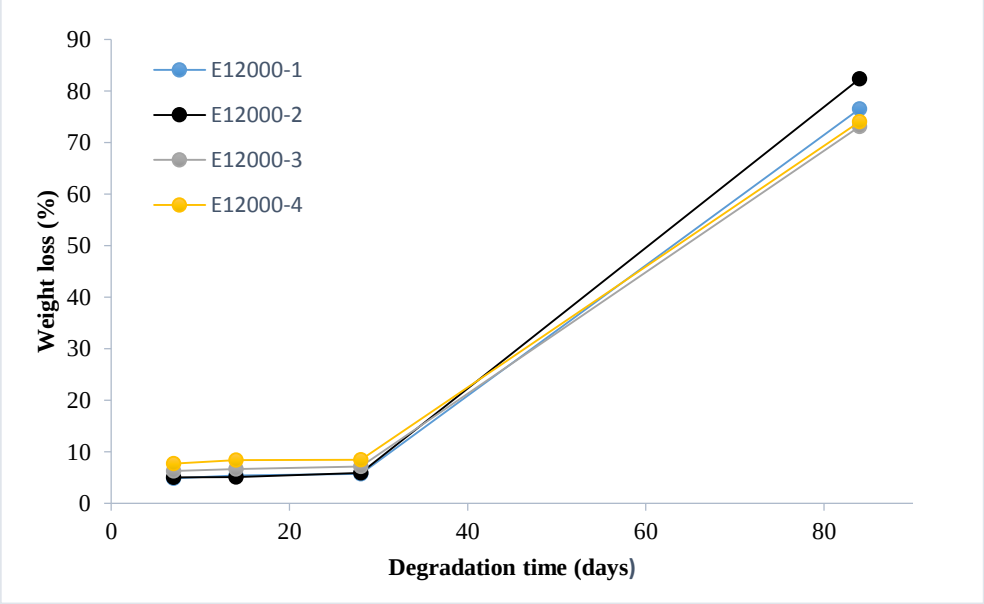

Figure 15: The weight loss for E_{12000} elastomers

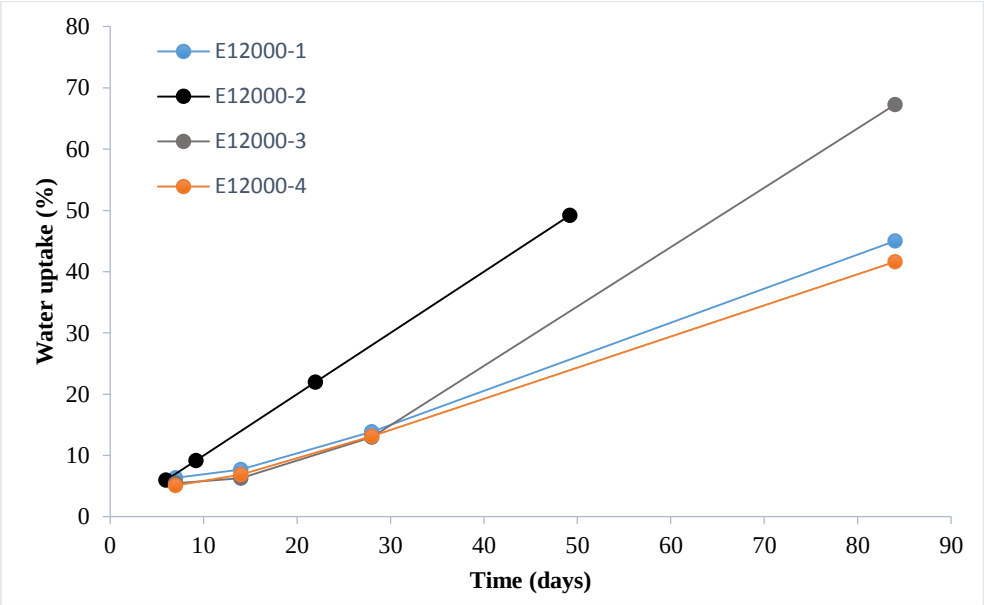

Figure 16: The water uptake for E_{12000} elastomers

As we can see from the results (Table IX) and plotted graphs, the initial water uptake as well as weight loss mainly depended on the molecular weight of used triblock copolymer and EO/LA ratio. For E_{4000} elastomers with higher EO/LA ratio (2.4), where less insoluble lactic units were included, the initial water uptake was more than 100%. After three months, those elastomers degraded completely. Consequently, it was impossible to estimate the hydrated weight, due to the difficulty to handle them (44). The higher degradation rates of E_{4000} elastomers compared to the E_{12000} ones could be ascribed to the higher EO/LA ratio. More hydrophilic unit chains of E_{4000} elastomers are able to soak water more intensively, which caused faster hydrolysis of PLA chains. Also, faster degradation of mentioned elastomers could be a consequence of higher amount of hydrophilic PEG units in the structure.

Table X: Water uptake and weight loss in PBS

Elastomer sample	Time (weeks)	Water uptake (%)	Weight loss (%)
$E_{4000\text{-}1}$	1	132 ± 6	5.7 ± 1.0
	2	154 ± 3	9.5 ± 0.6
	4	172 ± 5	19.8 ± 0.6
	12	525 ± 58	95.5 ± 1.7
$E_{4000\text{-}2}$	1	148 ± 1	6.4 ± 0.3
	2	185 ± 2	10.8 ± 0.5
	4	231 ± 9	21.4 ± 0.6
	12	/	100
$E_{4000\text{-}3}$	1	135 ± 4	6.8 ± 2.7
	2	165 ± 2	7.1 ± 3.1
	4	201 ± 11	14.1 ± 0.6
	12	/	99.9 ± 0.1
$E_{4000\text{-}4}$	1	146 ± 5	19.5 ± 4.7
	2	181 ± 9	14.2 ± 5.9
	4	241 ± 4	17.6 ± 0.8
	12	/	100
$E_{12000\text{-}1}$	1	6.3 ± 0.4	4.8 ± 0.6
	2	7.7 ± 0.4	5.4 ± 0.1
	4	13.9 ± 0.4	5.7 ± 0.1
	12	45.0 ± 7.9	76.5 ± 7.7
$E_{12000\text{-}2}$	1	5.9 ± 0.3	5.1 ± 0.3
	2	9.2 ± 0.9	5.1 ± 0.2
	4	21.9 ± 0.5	5.9 ± 0.2
	12	49.2 ± 8.2	82.4 ± 1.4
$E_{12000\text{-}3}$	1	5.5 ± 0.4	6.3 ± 0.4
	2	6.3 ± 0.5	6.7 ± 0.1
	4	12.9 ± 0.2	7.2 ± 0.2
	12	67.3 ± 12.2	73.1 ± 3.0
$E_{12000\text{-}4}$	1	5.1 ± 1.1	7.8 ± 0.5
	2	6.9 ± 0.2	8.4 ± 0.9
	4	13.1 ± 0.8	8.5 ± 0.3
	12	41.6 ± 9.2	74.0 ± 3.3

E_{12000} elastomers had lower EO/LA ratio (0.2), which resulted in lower hydrophilicity of those elastomers. Consequently, lower water uptake and weight loss were determined, compared to the E_{4000} elastomers. Lower and stable water uptakes as well as weight losses were observed during the first month for all elastomers. The initial weight loss was minimal, with insignificant change when different cross-linkers and photo-initiators were incorporated. According to our results, the higher the hydrophilicity of elastomers, the faster and more complete degradation was observed. As expected, the PETMP-based

elastomers expressed the highest weight loss and the water uptake due to the hydrophilicity of selected cross-linkers.

4.6 BIODEGRADATION PROFILE IN GLUTATHIONE AND PBS SOLUTION

In our study, bio-films prepared with DD, as a cross-linker, were tested in 10 μM solution of GSH in PBS (extracellular concentrations of GSH in health tissues). The water uptake and weight loss values during prescribed time period are shown in Figures 16 – 17 and in Table XI.

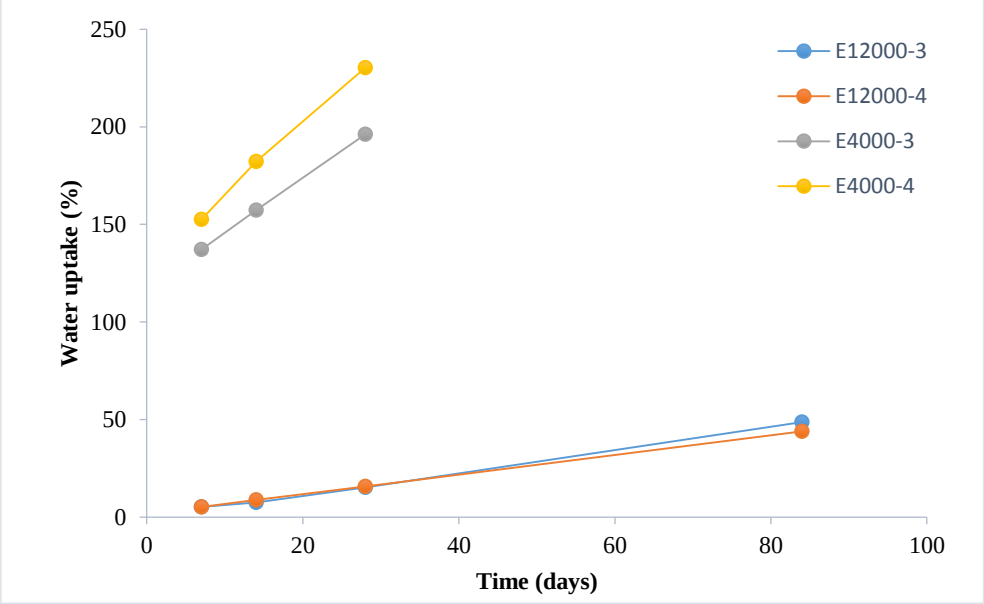

Figure 17: The water uptake in PBS/GSH

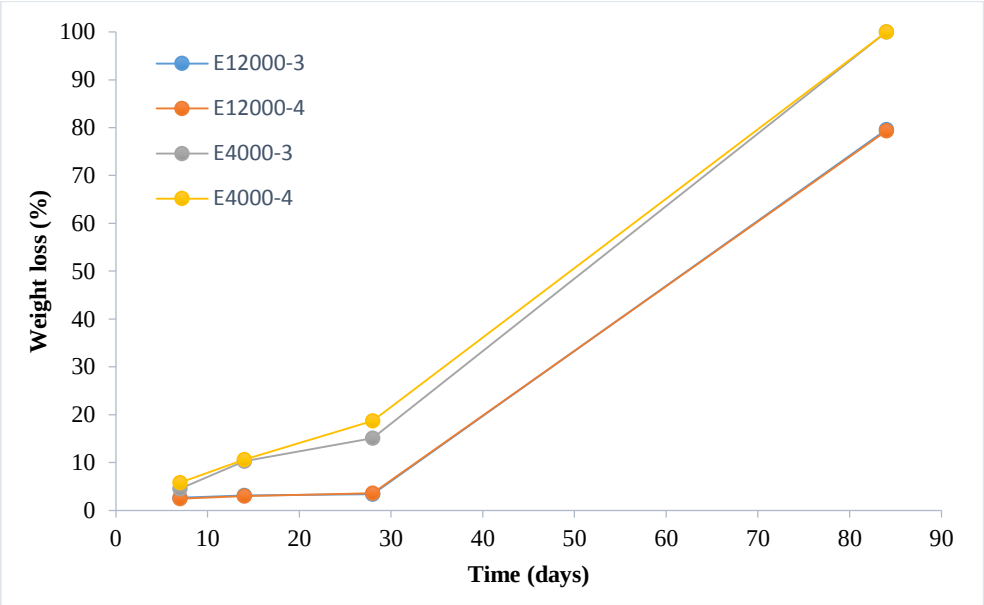

Figure 18: The weight loss in PBS/GSH

Table XI: Water uptake and weight loss in GSH and PBS.

Elastomer samples	Time (weeks)	Water uptake (%)	Weight loss (%)
E_{4000-3}	1	137 ± 9	4.5 ± 0.9
	2	157 ± 3	10.3 ± 4.6
	4	196 ± 7	15.1 ± 0.9
	12	/	100.0
E_{4000-4}	1	152 ± 6	5.8 ± 0.9
	2	182 ± 10	10.6 ± 1.1
	4	230 ± 14	18.7 ± 0.8
	12	/	100.00
$E_{12000-3}$	1	5.2 ± 0.2	2.7 ± 0.1
	2	7.4 ± 0.01	3.1 ± 0.1
	4	15.1 ± 0.3	3.4 ± 0.1
	12	48.7 ± 4.0	79.6 ± 2.6
$E_{12000-4}$	1	5.1 ± 0.5	2.5 ± 0.3
	2	8.7 ± 0.8	2.9 ± 0.3
	4	15.7 ± 1.1	3.6 ± 0.9
	12	43.8 ± 4.9	79.3 ± 4.4

No significant chance in results was observed in comparison to degradation tests in PBS only. Obtained results are not in accordance to literature data, where faster degradation of elastomers in the presence of GSH is expected to be observed.

5 CONCLUSION

Several thermoset biodegradable PLA-PEG-PLA based elastomers (E_{12000} and E_{4000} elastomers) were prepared by photo cross-linking. They were suitable as tissue scaffolds and could be easily prepared. The PLA-PEG-PLA triblock copolymers with different molecular weight and EO/LA ratio were used as a starting material. In the first step the preparation of photo cross-linkable triblock copolymers was reached by the reaction with the methacryloyl chloride. The methacrylation efficiency, calculated from the ^{1}H NMR spectrums was 66% for M-TBCP$_{12000}$, and 100% for M-TBCP$_{4000}$. In the second step, the biodegradable elastomers were prepared by photo cross-linking, where PETMP and DD were used as selected cross-linkers in different concentrations. All elastomers expressed high gel content (91%). E_{12000} elastomers had higher T_g (21 – 25 °C) compared to the E_{4000} elastomers (-46 °C). For all elastomers, T_g were below body temperature, which indicates appropriate mechanical properties of material under physiological conditions.

Mechanical properties of prepared elastomers were evaluated by tensile tests in dry and hydrated state, where the Young's modulus, ultimate tensile strength, ultimate strain and stress were determined. Mainly, the elastomer molecular weight had a significant impact on Young's modulus when compared to cross-linker nature. In dry state, E_{12000} elastomers had lower Young´s modulus and exhibited higher elasticity as E_{4000} elastomers, due to their longer chains and higher degree of bending. E_{4000} elastomers fractured more easily, which confirms their brittle character. The films were thinner, caused by the dense packing of molecules within the structure and consequently higher values of Young's modulus. DD-based E_{4000} elastomers were less elastic, due to the small sized molecule and less empty spaces within the structure. Higher ultimate strength, ultimate stress and ultimate strain were found in E_{12000} biofilms.

Statistical analyses with ANOVA confirmed no significant effect of hydration on Young's modulus for the most of the elastomers. The hydration had a significant effect on ultimate strain, tensile strength and stress. Determined mechanical properties are in accordance with literature data for elastomers used for biomedical applications (vascular vessels and myocardium).

Elastomer degradation profiles can be tailored by changing the EO/LA ratio and hydrophilicity/hydrophobicity of selected cross-linker. Elastomers with higher EO/LA ratio expressed higher initial water uptake and faster degradation. After three months, the degradation was complete for the majority of E_{4000} elastomers. PETMP as the selected cross-linker also caused higher water uptake and faster degradation, due to its hydrophilicity. All elastomers slowly degraded during the first month. After that period, a significant weight loss was observed. The degradation test in solution of GSH and PBS for DD-based elastomers showed no significant difference in the degradation profile.

Based on the mechanical properties and degradation profile, prepared elastomers could be used as scaffolds in soft tissue engineering applications, especially as nasal cartilage and ligaments.

6 LITERATURE

1. http://en.wikipedia.org/wiki/Tissue_engineering (accessed 2015, April 19; 21:09).
2. Chen Q, Liang S, Thouas GA: Elastomeric biomaterials for tissue engineering. Progress in polymer science 2013; 38: 584 – 671.
3. Langer R, Vacanti JP: Tissue engineering Science 1993; 260: 920 – 6.
4. Lee, CH, Shin HJ, Cho IH, Kang YM, Kim IA, Park KD, Shin JW: Nanofiber alignment and direction of mechanical strain affect the ECM production of human ACL fibroblast. Biomaterials 2005; 26: 1261 – 70.
5. Pelipenko J: Polymeric nanofibers: Development, evaluation and cell response. Doctoral thesis, University of Ljubljana, Faculty of pharmacy, Ljubljana, 2014: 33 – 34.
6. Burg KJL, Porter S, Kellam JF: Biomaterial developments for bone tissue engineering. Biomaterials 2000; 21: 2347 – 59.
7. Lanza RP, Langer R, Vacanti JP, editors. Principle of tissue engineering. 2nd ed, Academic Press, New York, 2000: 3 – 7.
8. Frantz C, Stewart KM, Weaver VM: The extracellular matrix at a glance. J Cell Sci 2010; 123: 4195 – 4200.
9. Pelipenko J, Kocbek P, Govedarica B, Rošic R, Baumgartner S, Kristl J: The topography of electrospun nanofibers and its impact on the growth and mobility of keratinocytes. Eur J Pharm Biopharm 2013; 84: 401 – 411.
10. Jankovic B, Pelipenko J, Škarabot J, Muševič I, Kristl J: The design trend in tissue-engineering scaffolds based on nanomechanical properties of individual electrospun nanofibers. Int J Pharm 2013; 455: 338 – 347.
11. Toh, YC, Ng S, Khong YM, Zhang X, Zhu Y, Lin PC, Te CM, Sun W, Yu H: Cellular responses to a nanofibrous environment. Nano Today 2006; 1: 34 – 43.
12. Williams DF, editor. Biomaterials: aims and scope. 2011 (accessed 2012, April 12; 19:09) http://www.elsevier.com/wps/find/journaldescription.cws_home/30392/description.
13. https://en.wikipedia.org/wiki/Biodegradable_polymer (accessed 2015, August 2; 18:45).
14. Williams D: Biomaterials and tissue engineering in reconstructive surgery. Sadhana 2003; 28: 563 – 74.
15. Nair LS, Laurencin CT: Biodegradable polymers as biomaterials. Progress in Polymer Science 2007; 32: 762 – 98.
16. Shalaby SW, Burg KJL: Absorbable and biodegradable polymers: contemporary topics. Boca raton, FL: CRC Press 2004: 159 – 90.
17. Domb AJ, Kost J, Wiseman DM, editors: Handbook of biodegradable polymers. Harwood Academic Publishers, Amsterdam, 1997: 544.
18. Piskin E: Biodegradable polymers as biomaterials. Journal of Biomaterials Science Polymer Edition 1995; 6: 775 – 95.

19. http://www.slideshare.net/shabeelpn/biomaterials-ceramics (accessed 2015, August 4; 19:48).
20. http://cdn.intechopen.com/pdfs-wm/18658.pdf (accessed 2015, August 4; 20:31).
21. Yoda R: Elastomers for biomedical applications. J. Biomater. Sci. Polymers Edition 1998; 9: 561 – 626.
22. Ghanbarzadeh B, Almasi H: Biodegradable polymers, Biodegradation – Life of Science, InTech, Rijeka, 2013: 141-74
23. Katti DS, Lakshmi S, Langer R, Laurencin CT: Toxicity, biodegradation and elimination of polyanhydrides. Adv Drug Deliv Rev 2002; 54: 933 – 61.
24. Lakshmi S. Naira, Cato T. Laurencin: Biodegradable polymers as biomaterials. Prog. Polym. Sci. 2007; 32: 762 – 798.
25. Ozdil D, Aydin HM: Polymers for medical and tissue engineering applications. J Chem Technol Biotechnol 2014; 89: 1793 – 1810.
26. Sell SA, Wolfe PS, Garg K, McCool JM, Rodriguez IA, Bowlin GL: The Use of Natural Polymers in Tissue Engineering: A Focus on Electrospun Extracellular Matrix Analogues. Polymers 2010; 2: 522 – 53.
27. Gunatillake PA, Adhikaru R: Biodegradable synthetic polymers for tissue engineering. European Cells and Materials 2003; 5: 1 – 16.
28. Rezwan K, Chen QZ, Blaker JJ, Boccaccini AR: Biodegradable and bioactive porous polymer/inorganic composite scaffolds for bone tissue engineering. Biomaterials 2006; 27: 3413 – 31.
29. BaoLin G, Ma P: Synthetic biodegradable functinal polymers for tissue engineering: a brief review. Science China Chemistry 2014; 57: 490 – 500.
30. Burkoth AK, Burdick J, Anseth KS: Surface and bulk modifications to photocrosslinked polyanhydrides to control degradation behavior. J Biomed Mater Res 2000; 51: 352 – 9.
31. Grenier S, Sandig M, Mequanint K: Polyurethane biomaterials for fabricating 3D porous scaffolds and supporting vascular cells. J Biomed Mater Res Part A 2007; 82: 802 – 9.
32. Bil M, Ryszkowska J, Roether JA, Bretcanu O, Boccaccini AR: Bioactivity of polyurethane-based scaffolds coated with Bioglass((R)). Biomed Mater 2007; 2: 93 – 101.
33. Hu XL, Chen XS, Xie ZG, Cheng HB, Jing XB: Aliphatic poly(estercarbonate) s bearing amino groups and its RGD peptide grafting. J Polym Sci Part A Polym Chem 2008; 46: 7022 – 32.
34. Xie ZG, Hu XL, Chen XS, Lu TC, Liu S, Jing XB: A biodegradable diblcok copolymer poly(ethylene glycol)-block-poly(l-lactide-co-2-methyl-2-carboxyl-propylene carbonate): docetaxel and RGD conjugation. J Appl Polym Sci 2008; 110: 2961 – 70.
35. Hemmrich K, Salber J, Meersch M, Wiesemann U, Gries T, Pallua N, Klee D. Three-dimensional nonwoven scaffolds from a novel biodegradable poly(ester amide) for tissue engineering applications. J Mater Sci Mater Med 2008; 19: 257 – 67.

36. Hsieh CY, Tsai SP, Wang DM, Chang YN, Hsieh HJ: Preparation of gamma-PGA/chitosan composite tissue engineering matrices. Biomaterials 2005; 26: 5617 – 23.
37. Yoshida H, Klinkhammer K, Matsusaki M, Moller M, Klee D, Akashi M: Disulfide-crosslinked electrospun poly(gamma-glutamic acid) nonwovens as reduction-responsive scaffolds. Macromol Biosci 2009; 9: 568 – 74.
38. Lin CY, Schek RM, Mistry AS, Shi XF, Mikos AG, Krebsbach PH, Hollister SJ: Functional bone engineering using ex vivo gene therapy and topology-optimized, biodegradable polymer composite scaffolds. Tissue Eng 2005; 11: 1589 – 98.
39. Lio Q, Jiang L, Shi R, Zhang L: Synthesis, preparation, in vitro degradation, and applications of novel degradable elastomers – A review. Progress in Polymer Science 2012; 37: 715 – 765.
40. Lloyd AW: Interfacial bioengineering to enhance surface biocompatibility. Med Device Technol 2002; 13: 18 – 21.
41. Amsden B: Curable biodegradable elastomers: emerging biomaterials for drug delivery and tissue engineering. Soft Matter 2007; 3: 135 – 48.
42. Bettinger CJ, Bruggeman JP, Borenstein JT, Langer RS: Amino alcohol-based degradable poly(ester amide) elastomers. Biomaterials 2008; 29: 2315 – 25.
43. Amsden BG, Tse MY, Turner ND; Knight DK, Pang SC: In vivo degradation behaviour of photo-cross-linked star (epsilon-caprolactone-co.D,L.lactide) elastomers. Biomacromolecules 2006; 7: 365 – 72.
44. Harrane A., Leroy A., Nouailhas H., Garric X., Coudane J. and Nottelet B: PLA-based biodegradable and tunable soft elastomers for biomedical applications. Biomedical Materials 2011; 6: 1 – 11.
45. Younes HM, Bravo-Grimaldo E, Amsden BG: 2004 Synthesis, characterization and in vitro degradation of a biodegradable elastomers. Biomaterials 2004; 25: 5261 – 9.
46. Cohn D, Salomon AF: Designing biodegradable multiblock PCL/PLA thermoplastic elastomers. Biomaterials 2005; 26: 2297 – 305.
47. Stankus JJ, Guan JJ and Wagner WR: Fabrication of biodegradable elastomeric scaffolds with sub-micron morphologies. J. Biomed. Mater. Res. 2004; 70: 603–14.
48. Brown AH, Sheares VV: Amorphous unsaturated aliphatic polyesters derived from dicarboxylic monomers synthesized by Diels-Alder chemistry. Macromolecules 2007; 40: 4848 – 53.
49. Cohn D, Stern T, Gonzalez MF, Epstein J: Biodegradable poly(ethylene oxide)/ poly(epsilon-caprolactone) multiblock copolymers. J Biomed Mater Res 2002; 59: 273 – 81.
50. Kylma J, Seppala JV: Synthesis and characterization of a biodegradable thermoplastic poly(ester-urethane) elastomer. Macromolecules 1997; 30: 2876 – 82.
51. Jiang X, Li J H, Ding M M, Tan H, Ling Q Y, Zhong Y P and Fu Q: Synthesis and degradation of nontoxic biodegradable waterborne polyurethanes elastomer with

poly(epsilon-caprolactone) and poly(ethylene glycol) as soft segment. Eur. Polym. J. 2007; 43: 1838 – 46.
52. Wang WS, Ping P, Yu H J, Chen XS, Jing XB: Synthesis and characterization of a novel biodegradable, thermoplastic polyurethane elastomer. J Polym Sci 2006; 44: 5505 – 12.
53. Zeng JB, Li YD, Zhu QY, Yang KK, Wang XL, Wang YZ: A novel biodegradable multiblock poly(ester urethane) containing poly(L-lactic acid) and poly(butylene succinate) blocks. Polymer 2009; 50: 1178 – 86.
54. Barrett DV, Luo W, Yousaf MN: Aliphatic polyester elastomers derived from erythritol and α,ω-diacids. Polym. Chem. 2010; 1: 296 – 302.
55. Helminen AO, Korhonen H, Seppala JV: Structure modification and crosslinking of methacrylated polylactide oligomers J. Appl. Polym. Sci. 2002; 86: 3616–24.
56. Dey J, Xu H, Shen JH, Thevenot P, Gondi SR, Nguyen KT, Sumerlin BS, Tang LP, Yang J: Development of biodegradable crosslinked urethane-doped polyester elastomers Biomaterials 2008; 29: 4637 – 49.
57. Helminen AO, Korhonen H, Seppala JV: Structure modification and crosslinking of methacrylated polylactide oligomers J Appl Polym Sci 2002; 86: 3616 – 24.
58. Bat E, Kooten TG, Feijen J, Grijpma DW: Resorbable elastomeric networks prepared by photo-crosslinking of high-molecular weight poly(trimethylene carbonate) macromers as crosslinking aids. Acta Biomaterials 2011; 7: 1939 – 48.
59. Bettinger CJ. Synthesis and microfabrication of biomaterials for soft-tissue engineering. Pure Appl Chem 2009; 81: 2183 – 201.
60. https://en.wikipedia.org/wiki/Polylactic_acid (accessed 2015, August 4; 22:49).
61. Yang SF, Leong KF, Du ZH, Chua CK: The design of scaffolds for use in tissue engineering Part 1. Traditional factors. Tissue Eng 2001; 7: 679 – 89.
62. Wan Y, Chen W, Yang J, Bei J, Wang S: Biodegradable poly(l-lactide)-poly(ethylene glycol) multiblock copolymer: synthesis and evaluation of cell affinity. Biomaterials 2003; 24: 2195 – 2203.
63. Garlotta, D: A literature review of poly(lactic acid). J Polym Environ 2001; 9: 63 – 84.
64. Anderson KS, Schreck KM, Hillmyer MA: Toughening polylactide. Polym Rev *2008;* 48: 85 – 108.
65. Xiao L, Wang B, Yang G, Gauthier M: Poly(Lactic Acid)-Based Biomaterials: Synthesis, Modification and Applications. Biomedical Science, Engineering and Technology, InTech, Rijeka, 2012: 248 – 271.
66. http://www.chemistry.illinois.edu/research/organic/seminar_extracts/2005_2006/06_Porter.pdf (accessed 2015, August 4; 23:04).
67. Yang SF, Leong KF, Du ZH, Chua CK: The design of scaffolds for use in tissue engineering Part 1. Traditional factors. Tissue Eng 2001; 7: 679 – 89.
68. Lanza RP, Langer R, Chick WL, editors. Principle of tissue engineering. Academic Press Landes, 1996: 263 – 72.

69. Dey J, Xu H, Shen JH, Thevenot P, Gondi SR, Nguyen KT, Sumerlin BS, Tang LP, Yang J: Development of biodegradable crosslinked urethane-doped polyester elastomers. Biomaterials 2008; 29: 4637 – 49.
70. Shen JY, Pan XY, Lim CH, Chan-Park MB, Zhu X, Beuerman RW: Synthesis, characterization, and in vitro degradation of a biodegradable photo-cross-linked film from liquid poly(epsilon-caprolactone-co-lactide-coglycolide) diacrylate. Biomacromolecules 2007; 8: 376 – 85.
71. Mosnacek J, Yoon JA, Juhari A, Koynov K, Matyjaszewski K: Synthesis, morphology and mechanical properties of linear triblock copolymers based on poly(alpha-methylene-gamma-butyrolactone). Polymer 2009; 50: 2087 – 94.
72. Shields R, Harris J, Davis M: Suitability of poly(ethylene glycol) blocks) as dilution indicator in the human colon, J Controlled Release Gastroenterology 1968; 54: 331 – 333.
73. Kumar N, Ravikumar NVM, Domb AJ: Biodegradable block copolymers. Advanced Drug Delivery Reviews 2001; 53: 23 – 44.
74. Mason MN, Metters AT, Bowman CN, Anseth KS: Predicting controlled-release behavior of degradable PLA-b-PEG-b-PLA hydrogels. Macromolecules 2001; 34: 4630 – 5.
75. Sanabria-DeLong N, Crosby AJ and Tew GN: Photo-cross-linked PLA-PEO-PLA hydrogels from self-assembled physical networks: mechanical properties and influence of assumed constitutive relationships, Biomacromolecules 2008; 9: 2784 – 91.
76. Drotleff S, Lungwitz U, Breunig M, Dennis A, Blunk T, Tessmar J, Gopferich A: Biomimetic polymers in pharmaceutical and biomedical science. Eur J Pharm Biopharm 2004; 58: 385 – 407.
77. Shin H, Jo S, Mikos AG: Biomimetic materials for tissue engineering. Biomaterials 2003; 24: 4353 – 64.
78. Pan J: Modelling Degradation of Bioresorbable Polymeric Medical Devices. Woodhead Publishing, Cambridge, 2015: 4 – 5.
79. Nair LS, Laurencin ST: Biodegradable polymers as biomaterials. Prog Polym Sci 2007; 32: 762 – 98.
80. Gopferich A: Mechanisms of polymer degradation and erosion. Biomaterials 1996; 17: 103 – 14.
81. Langer RS., Peppas NA: Present and future applications of biomaterials in controlled drug delivery system. Biomaterials 1981; 2: 201 – 14.
82. https://en.wikipedia.org/wiki/Surface_and_bulk_erosion (accessed 2015, August 31; 23:38).
83. Lee JW, Gardella JA: In vitro hydrolytic surface degradation of poly (glycolic acid): role of the surface segregated amorphous region in the induction period of bulk erosion. Macromolecules 2001; 34: 3928 – 37.
84. Zustiak SP, Leach JB: Hydrolytically degradable poly(ethylene glycol) hydrogel scaffolds with tunable degradation and mechanical properties. Biomacromolecules 2010; 11: 1348 – 57.

85. Hayashi K. Nakamura T: Material test system for the evaluation of mechanical properties of biomaterials. J Biom Mat Res 2004; 19: 133 – 44.
86. https://en.wikipedia.org/wiki/Tensile_testing (accessed 2015, August 1; 21:45).
87. http://eng.sut.ac.th/metal/images/stories/pdf/Lab_3Tensile_Eng.pdf (accessed 2015, August 1; 22:21).
88. http://www.engr.sjsu.edu/sgleixner/PRIME/Sports/Class%203_4/Class%203_4_polymer_mech_prop.pdf (accessed 2015, July 21; 23:44).
89. http://people.virginia.edu/~lz2n/mse209/Chapter15c.pdf (accessed 2015, July 21: 23:59).
90. Egart M: Evaluation of structural mechanical properties of active pharmaceutical ingredients with instrumented nanoindentation and their importance for tablets compression. University of Ljubljana, Faculty of Pharmacy, Ljubljana 2014: 13 – 16.
91. http://en.wikipedia.org/wiki/Young%27s_modulus (accessed 2015, August 15; 23:11).
92. https://en.wikipedia.org/wiki/Strength_of_materials (accessed 2015, August 15).
93. http://www.britannica.com/EBchecked/topic/654186/Youngs-modulus (accessed 2015, August 15; 23:46).
94. http://en.wikibooks.org/wiki/Alevel_Physics_%28Advancing_Physics%29/Stress,_Strain_%26_Young%27s_Modulus (accessed 2015, August 15; 23:59).
95. http://people.virginia.edu/~lz2n/mse209/Chapter15c.pdf (accessed 2015, July 22 17:31).
96. https://en.wikipedia.org/wiki/Ultimate_tensile_strength#Typical_tensile_strengths (accessed 2015, July 22; 17:58).
97. http://en.wikipedia.org/wiki/Size-exclusion_chromatography (accessed 2015, July 22; 20:19).
98. http://www.chem.agilent.com/Library/technicaloverviews/Public/5990-7890EN.pdf (accessed 2015, April 8; 20:21).
99. http://www.shimadzu.com/an/hplc/support/lib/lctalk/55/55intro.html (accessed 2015, April 9; 19:43).
100. https://www.chem.agilent.com/Library/primers/Public/5990-6969EN%20GPC%20SEC%20Chrom%20Guide.pdf (accessed 2015, April 9; 22:31).
101. https://en.wikipedia.org/wiki/Molar_mass_distribution#Number_average_molar_mass (accessed 2015, August 31; 21:37).
102. https://en.wikipedia.org/wiki/Molar_mass_distribution#Number_average_molar_mass (accessed 2015, August 31; 22:02).
103. Hansen JM, Harris C: Glutathione during embryonic development. Biochimica et Biophysica Acta (BBA) – General Subjects, 2015, 1850: 1527-1542.
104. Traverso N, Ricciarelli R, Nitti M, Marengo B, Furfaro AL, Pronzato MA, Marinari UA, Domenicotti C: Role of Glutathione in Cancer Progression and Chemoresistance. Oxidative Medicine and Cellular Longevity 2013; 2013: 1-10.

105. http://www.canceractive.com/cancer-active-page-link.aspx?n=3150 (accessed 2015, June 4; 22:05).
106. Cheng R, Feng F, Meng F, Deng C, Feijen J, Zhong J: Glutathione-responsive nano-vehicles as a promising platform for targeted intracellular drug and gene delivery. Controlled Release 2011: 152: 2 – 12.
107. Dufort S, Sancey L, Coll JL: Physico-chemical parameters that govern nanoparticles fate also dictate rules for their molecular evolution. Adv Drug Delivery Rev 2012; 64: 179 – 189.
108. Huo M, Yuan J, Taob L, Wei Y: Redox-responsive polymers for drug delivery: from molecular design to applications. Polym Chem 2014; 5: 1519.
109. Wan Y, Chen W, Yang J, Bei J, Wang S: Biodegradable poly(l-lactide)-poly(ethylene glycol) multi-block copolymer synthesis and evaluation of cell affinity. Biomaterials 2003; 24: 2195 – 2203.
110. Cohn D, Pines E, Hotovely A: Methods or compositions for reducing or eliminating post-surgical adhesion formation. United States Patent, Patent number 10, 749, 436, date of patent April 10, 2007.
111. Li F, Li SM, Vert M: Synthesis and rheological properties of polylactide/poly (ethylene glycol) multiblock copolymers. Macromol Biosci 2005; 5: 1125 – 31.